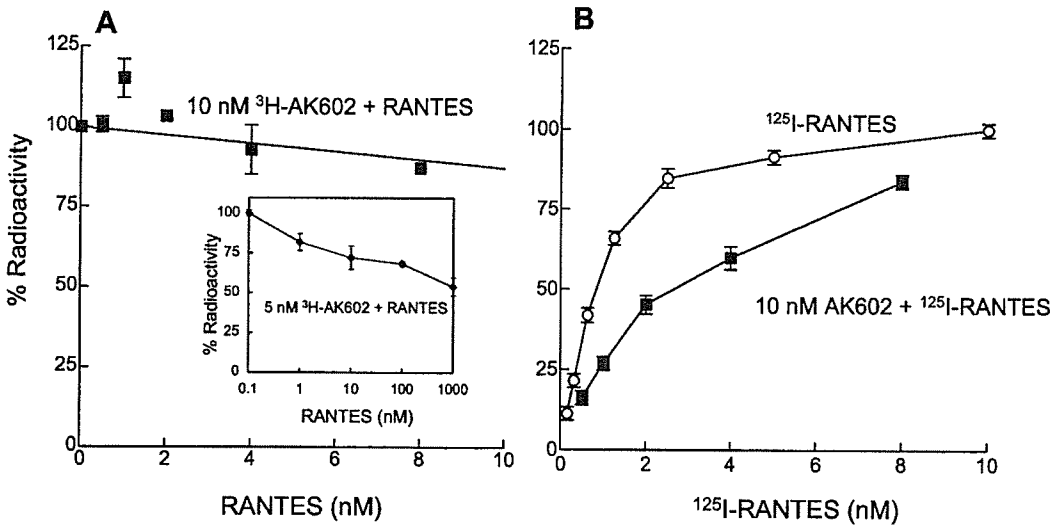

FIG. 6. AK602 and RANTES bind simultaneously to CCR5. (A) CCR5$^+$ CHO cells were exposed to 10 nM [^{3}H]AK602 and various concentrations of unlabeled RANTES. After 1 h of incubation, the cells were washed, and the [^{3}H]AK602 bound to the cells was measured. Note that 100% radioactivity on the ordinate denotes the radioactivity of cell-bound [^{3}H]AK602 without RANTES and that ≈90% of CCR5 molecules are bound to AK602 at 10 nM (Fig. 3A). (B) CCR5$^+$ CHO cells were exposed to 10 nM unlabeled AK602 and various concentrations of [^{125}I]RANTES. After 1 h of incubation, the cells were washed, and the [^{125}I]RANTES bound to the cells was measured. The binding profile of [^{125}I]RANTES alone is illustrated by open circles. Note that 100% radioactivity is equated to the radioactivity of cell-bound [^{125}I]RANTES at 10 nM. The K_d values of RANTES in the presence and absence of 10 nM AK602 were 4.5 and 0.6 nM, respectively.

though conformational changes potentially caused by either of the two might have occurred. Indeed, 15 to 25% inhibition was seen at nearly equimolar concentrations of AK602 and RANTES, which may reflect the involvement of the conformational changes caused by either of the two agents or an overlap in their binding sites (or domains).

AK602 permits RANTES-induced chemotaxis and CCR5 internalization at anti-HIV-1 activity-exerting concentrations. We next asked whether AK602 allowed RANTES-induced chemotaxis and CCR5 internalization with CCR5$^+$ MOLT4 cells and CCR5$^+$ CHO cells at its anti-HIV-1 activity-exerting concentrations. As shown in Fig. 7A, AK671/SCH-C most potently blocked chemotaxis, followed by E921/TAK-779. The chemotaxis values at the IC_{50}s against R5 HIV-1_{Ba-L} of AK671/SCH-C and E921/TAK-779 (4 and 24 nM, respectively: Table 1) were low, 18 and 8%, respectively, suggesting that these two inhibitors considerably blocked chemotaxis at their anti-HIV-1 IC_{50} concentrations as determined in peripheral blood mononuclear cells. In contrast, the chemotaxis seen at the IC_{50} level of AK602, 0.4 nM (see Table 1), was considerable, with 70% retained (Fig. 7A), while that seen AK530 was much less (30%).

In order to corroborate the modest chemotaxis inhibition seen with AK602, the inhibition of RANTES-induced CCR5 internalization was also examined. In the absence of CCR5 inhibitors, ≈50% of CCR5 molecules were internalized from the surface of CCR5$^+$ CHO cells incubated for 1 h at 37°C in the presence of 10 nM RANTES; however, AK671/SCH-C and E921/TAK-779 at 100 nM considerably blocked internalization, and only 19 and 6%, respectively, of CCR5 molecules were internalized. In the presence of higher concentrations of AK671/SCH-C and E921/TAK-779, 300 and 1,000 nM, virtually no CCR5 internalization occurred (Fig. 7B). In contrast, AK530 and AK602 at 100 nM allowed RANTES-induced CCR5 internalization of 46 and 30%, respectively, and even at 300 and 1,000 nM, 10 to 34% CCR5 internalization occurred (Fig. 7B).

DISCUSSION

A novel SDP derivative, AK602/ONO4128/GW873140, exhibited high affinity to CCR5, blocked rgp120/sCD4 complex binding to CCR5, and exerted potent activity against a wide spectrum of laboratory and primary R5 HIV-1 isolates, including HIV-1_{MDR}. We recently examined AK602 against several non-clade B R5 HIV strains and found that in general AK602 is comparably active against such non-clade B strains (data not shown). It is of note that several small-molecule CCR5 inhibitors have been reported in the literature, including SCH-D (D. Schurmann et al., Abstr. 11th Conf. Retroviruses Opportunistic Infections, 2004, abstr. 140LB), UK427,857 (A. L. Pozniak et al. Abstr. 43rd Intersci. Conf. Antimicrob. Agents Chemother., 2003, abstr. H-443), CMPD167 (32), and TAK-220 (Y. Iizawa et al., Abstr. 10th Conf. Retroviruses Opportunistic Infections, 2003, abstr. 11).

In the present study, we also demonstrated that AK602 potently blocked rgp120/sCD4 complex binding to CCR5. With respect to gp120/CD4 binding to CCR5, Olson et al. previously reported no correlation between fusion with and entry into the target cell of HIV-1 and inhibition of rgp120/sCD4 complex binding to CCR5, based on data with various anti-CCR5 monoclonal antibodies (24). However, with all small-molecule SDP derivatives examined in the present study, inhibition of HIV-1 infectivity and replication generally correlated with inhibition of the rgp120/sCD4 complex binding to CCR5, strongly suggesting that the anti-HIV-1 activity of SDP

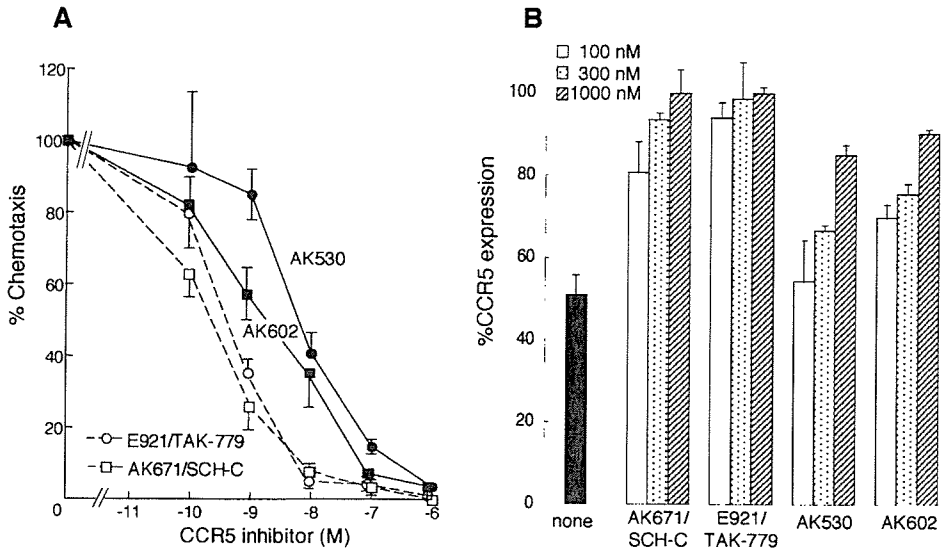

FIG. 7. AK602 allows RANTES-induced chemotaxis and CCR5 internalization. (A) $CCR5^+$ MOLT4 cells were exposed to various concentrations of AK530, AK602, E921/TAK-779, or AK671/SCH-C, thoroughly washed, plated onto the upper chamber of the ChemTx System, exposed to 0.5 nM RANTES contained in the lower chamber, and incubated for 4 h; the number of the cells which migrated to the lower chamber was determined, and chemotaxis was calculated. (B) $CCR5^+$ CHO cells were exposed to 10 nM RANTES in the presence or absence of various concentrations of each CCR5 inhibitor and washed with acidic solution for removal of the cell-bound RANTES (21). The amount of cell surface CCR5 was subsequently determined with monoclonal antibody 3A9 (BD PharMingen), which recognizes the N terminus of CCR5 and competes with none of the CCR5 inhibitors tested. In panel A, the level of chemotaxis suppression by TAK-779 and SCH C was greater than that by AK530 and AK602 at four concentrations examined, although complete suppression was seen only at the highest concentration of the AK compounds, 1 μM. However, in panel B, the level of CCR5 internalization suppression by TAK-779 and SCH-C was greater than that of the AK compounds at all three concentrations examined.

derivatives stems from their inhibition of gp120 binding to CCR5, as reported for other CCR5 inhibitors such as TAK-779 (3), although the binding pocket (or subsite) of CCR5 for certain SDP derivatives (such as AK530) apparently does not quite overlap the rgp120/sCD4 complex binding site of CCR5 (Fig. 3B). It is also possible that the conformational changes ensuing upon AK602's binding to CCR5 could differ from that ensuing upon AK530's binding to CCR5, thereby producing differences in gp120/sCD4 binding and anti-HIV activity.

It is generally noted that although the determination of any binding sites with antibodies provides "indirect" evidence, in many cases it gives good insights (14). Indeed, SCH-C has been reported to induce conformational changes in CCR5 and bind to its transmembrane (TM) domain, thereby blocking HIV-gp120 binding to CCR5. In our data, SCH-C completely blocked the binding of the "multidomain"-reactive monoclonal antibody 45523, which reportedly causes conformational changes in CCR5, while it only moderately blocked the binding of the ECL2B-specific monoclonal antibody 45531 (Fig. 4). In contrast, AK602 completely blocked the binding of both 45523 and 45531. Considering that monoclonal antibody 45531's CCR5 binding is closely linked to amino acids 184 to 189 of ECL2B, as shown by Lee and colleagues (14), it was thought that the binding site of AK602 includes ECL2B or is vicinal to it. Indeed, our recent analysis with the alanine-scanning algorithm showed that AK602 totally failed to bind to a CCR5 mutant when a K191A substitution was introduced (Maeda et al., unpublished data), corroborating and extending the idea that AK602's binding site involves the ECL2B domain.

It is noted that the IC_{50} of AK602 against HIV-1 as determined in peripheral blood mononuclear cells (0.4, 0.1, and 0.2 nM against $HIV\text{-}1_{Ba\text{-}L}$, $HIV\text{-}1_{JR\text{-}FL}$, and $HIV\text{-}1_{MOKW}$, respectively: Table 1) are substantially lower than the K_d of AK602 (2.9 nM) and the IC_{50} of AK602 for its inhibition of rgp120/sCD4 complex binding to CCR5 (2.7 nM). The anti-HIV-1 IC_{50}s of AK602 are also lower than the IC_{50}s of AK602 for its inhibition of MIP-1α-induced Ca^{2+} influx (39.8 nM; unpublished data) and that for its inhibition of CCR5 internalization (≈300 nM; unpublished data).

One possible explanation for these inconsistencies is the different cell lines employed for each assay. However, it is of note that when we determined the IC_{50} values against several R5 HIV strains and K_d values of AK602 in MAGI/CCR5 cells (18), AK602's IC_{50}s (≈0.2 nM) were reproducibly lower than AK602's K_d (3.8 nM) (data not shown). Thus, one can postulate that for the inhibition of HIV-1 infection by CCR5 inhibitors, not all CCR5 molecules might have to be occupied. In this regard, our studies with ^3H-labeled AK602 and $CD4^+$ target cells expressing CCR5, MAGI/CCR5 (18) and U373-MAGI (34), have shown that less than 30% of HIV-1 infection occurred when approximately 50% of CCR5 molecules were bound by AK602, and at its anti-HIV-1 IC_{50} concentration, AK602 was found to bind to 5 to 20% of CCR5 molecules on the target cells (Maeda et al., unpublished data). These data suggest that when one of the multimerized CCR5 molecules is bound or occupied by AK602, inhibition of the cell is likely to be blocked, although further stoichiometric analyses need to be conducted.

It has been thought that individuals carrying a gene encoding a mutant form of CCR5 called Delta32 are resistant to HIV-1

infection and apparently do not have significant health problems (2, 15, 23, 25). One can assume that individuals with homozygous CCR5-Delta32 might inherently have certain defenses which could compensate for the deficiency of CCR5. In this regard, there has been a report that individuals carrying homozygous CCR5-Delta32 have longer survival of renal transplants than those with other genotypes, suggesting that such individuals might have compromised graft rejection immunity (7). Moreover, Woitas et al. have reported that individuals with homozygous CCR5-Delta32 have significantly higher levels of hepatitis C virus in blood than their counterparts who have wild-type CCR5, suggesting that the CCR5-Delta32 mutation may be an adverse host factor in hepatitis C virus infection (35), although others have recently argued against a role of CCR5 in susceptibility to hepatitis C virus infection or response to antiviral therapy (9). Thus, sustained, long-term suppression of the effect of CC-chemokines/CCR5 interactions, in particular in those who carry wild-type CCR5 and might not have a possible compensatory mechanism for the absence of CCR5, might produce adverse effects, and caution should be used in the development of chemokine receptor antagonists as potential therapeutics for HIV-1 infection.

In this respect, SDP derivatives such as AK602 can preserve CC-chemokine/CCR5 interactions at their anti-HIV activity-exerting concentrations; they allow RANTES and MIP-1β binding to $CCR5^+$ cells and their functions at anti-HIV-1 concentrations. In contrast, two previously published CCR5 inhibitors, TAK-779 and SCH-C, fully blocked CC-chemokine/CCR5 interactions (Fig. 5 and 7). It is of note that AK602's complete inhibition of the binding of MIP-1α was not surprising because in the initial search of lead compounds, we sought compounds that blocked the binding of ^{125}I-labeled MIP-1α to $CCR5^+$ CHO cells and MIP-1α-elicited cellular Ca^{2+} mobilization, as described previously (17).

In support of the above observation, the results of competitive biding assays with [^{3}H]AK602 and [^{125}I]RANTES and their corresponding unlabeled agents clearly indicated that AK602 and RANTES bind simultaneously to CCR5 (Fig. 6). Moreover, AK602 allowed $CCR5^+$ MOLT4 cells to undergo RANTES-elicited chemotaxis (Fig. 7A) and $CCR5^+$ CHO cells to internalize CCR5 in response to RANTES (Fig. 7B) at concentrations much greater than AK602's anti-HIV-1 activity-exerting concentration in peripheral blood mononuclear cells. However, it is worth noting that although AK602 blocked the binding of [^{125}I]RANTES to $CCR5^+$ CHO cells only by ≈40% at micromolar concentrations (Fig. 5A), it virtually completely blocked the RANTES-induced chemotaxis at micromolar concentrations, as examined in $CCR5^+$ MOLT4 cells (Fig. 7A). This apparent inconsistency could be explained by the different cell lines employed for each assay and the fact that the number of CCR5 molecules in $CCR5^+$ CHO cells (≈5×10^5/cell) is substantially different from that of $CCR5^+$ MOLT4 cells (≈1×10^5/cell), and thus, AK602 could more efficiently block the chemotaxis of MOLT4 cells. It is also possible that AK602 may more effectively block CCR5 multimerization, which is reportedly important for the functionality of the G protein-coupled receptor (29), rather than the RANTES binding block to CCR5 per se. However, it is not clear yet whether AK602's unique profile that AK602 partially allows RANTES and MIP-1β to bind to CCR5 despite AK602's tight binding to CCR5 brings about a clinical advantage. This can be examined only in the setting of clinical trials and careful clinical investigation in long-term treatment with such an agent.

Several HIV-1 variants which acquired resistance to CC-chemokines, including MIP-1α and CCR5 inhibitors, have been reported. Trkola et al. described that when HIV-1 was passaged in the presence of increasing concentrations of a CCR5-specific, structurally SCH-C-related CCR5 inhibitor, AD101, an escape mutant which contained 22 amino acid substitutions in the gp120 subunits emerged as early as after 19 passages (31). This escape mutant showed a >20,000-fold resistance to AD101 and was similarly resistant to SCH-C compared with wild-type HIV-1, suggesting that HIV-1 can acquire the capability of using CCR5 bound to certain classes of CCR5 inhibitors for its entry into the target cell (31). Maeda et al. reported that HIV-$1_{JR\text{-}FL}$, following in vitro selection against MIP-1α over 3 months, acquired amino acid substitutions in the V2 and V3 regions of HIV-1 gp120 and became four- to sixfold more resistant to MIP-1α, MIP-1β, and RANTES (18). In this regard, as of this writing, we have passaged HIV-$1_{Ba\text{-}L}$ in $CD4^+$ $CCR5^+$ PM1 cells (16) in the presence of moderately increasing concentrations of AK602 in one selection experiment and aggressively increasing concentrations of AK602 in another selection experiment over 22 months (45 passages); however, the virus has acquired no detectable resistance to AK602 and no significant amino acid substitutions (Nakata et al., unpublished data).

It is worth noting that the anti-HIV-1 activity of AK602 is virtually unaffected by the presence of human serum proteins. For instance, the IC_{50} of AK602 against HIV-$1_{Ba\text{-}L}$ in the presence of 10% fetal calf serum in culture medium was 0.4 ± 0.3 nM, while those of AK602 with 10 μM α1-acid glycoprotein and 45% human serum added to the culture medium were 0.8 ± 0.3 and 0.7 ± 0.7 nM, respectively. AK602 failed to induce Ca^{2+} flux, chemotaxis, or CCR5 internalization in $CCR5^+$ cells (Maeda et al., unpublished data). As far as the sensitivities of our methods used in the present work, AK602 is to be categorized as a nonagonist or antagonist. The phase 1 clinical trial of AK602 in HIV-1-seronegative individuals has recently been concluded, and no significant adverse effects have been documented. Considering that AK602 potently inhibited the replication of HIV-1 in vitro and in a nonobese diabetic-SCID mouse model (Nakata et al., unpublished data) and that AK602 has a favorable oral bioavailability in rodents, averaging 20 to 30% (unpublished data), the present data strongly suggest that AK602 is a promising CCR5 inhibitor as a potential therapeutic for HIV-1 infection.

ACKNOWLEDGMENTS

We thank Steve LaFon, Larry Boone, Jim Demarest, Eddy Arnold, Shigeyoshi Harada, Kazuhisa Yoshimura, and Yosuke Maeda for helpful discussion and critical reading of the manuscript.

This work was supported in part by a grant from the Research for the Future Program (JSPS-RFTF 97L00705) of the Japan Society for the Promotion of Science, a Grant-in-Aid for Scientific Research (Priority Areas) from the Ministry of Education, Culture, Sports, Science, and Technology of Japan (Monbu-Kagakusho), and a Grant for the Promotion of AIDS Research from the Ministry of Health, Welfare, and Labor of Japan (Kosei-Rohdosho).

REFERENCES

1. **Baba, M., O. Nishimura, N. Kanzaki, M. Okamoto, H. Sawada, Y. Iizawa, M. Shiraishi, Y. Aramaki, K. Okonogi, Y. Ogawa, K. Meguro, and M. Fujino.** 1999. A small-molecule, nonpeptide CCR5 antagonist with highly potent and selective anti-HIV-1 activity. Proc. Natl. Acad. Sci. USA **96:**5698–5703.
2. **Dean, M., M. Carrington, C. Winkler, G. A. Huttley, M. W. Smith, R. Allikmets, J. J. Goedert, S. P. Buchbinder, E. Vittinghoff, E. Gomperts, S. Donfield, D. Vlahov, R. Kaslow, A. Saah, C. Rinaldo, R. Detels, and S. J. O'Brien.** 1996. Genetic restriction of HIV-1 infection and progression to AIDS by a deletion allele of the CKR5 structural gene. Hemophilia Growth and Development Study, Multicenter AIDS Cohort Study, Multicenter Hemophilia Cohort Study, San Francisco City Cohort, ALIVE Study. Science **273:**1856–1862.
3. **Dragic, T., A. Trkola, D. A. Thompson, E. G. Cormier, F. A. Kajumo, E. Maxwell, S. W. Lin, W. Ying, S. O. Smith, T. P. Sakmar, and J. P. Moore.** 2000. A binding pocket for a small molecule inhibitor of HIV-1 entry within the transmembrane helices of CCR5. Proc. Natl. Acad. Sci. USA **97:**5639–5644.
4. **Evans, E. A.** 1974. Catalytic exchange in solution, p. 271–317. *In* Tritium and its compounds. Wiley and Sons, New York, N.Y.
5. **Fauci, A. S.** 2003. HIV and AIDS: 20 years of science. Nat. Med. **9:**839–843.
6. **Finzi, D., J. Blankson, J. D. Siliciano, J. B. Margolick, K. Chadwick, T. Pierson, K. Smith, J. Lisziewicz, F. Lori, C. Flexner, T. C. Quinn, R. E. Chaisson, E. Rosenberg, B. Walker, S. Gange, J. Gallant, and R. F. Siliciano.** 1999. Latent infection of $CD4^+$ T cells provides a mechanism for lifelong persistence of HIV-1, even in patients on effective combination therapy. Nat. Med. **5:**512–517.
7. **Fischereder, M., B. Luckow, B. Hocher, R. P. Wuthrich, U. Rothenpieler, H. Schneeberger, U. Panzer, R. A. Stahl, I. A. Hauser, K. Budde, H. Neumayer, B. K. Kramer, W. Land, and D. Schlondorff.** 2001. CC chemokine receptor 5 and renal-transplant survival. Lancet **357:**1758–1761.
8. **Gartner, S., P. Markovits, D. M. Markovitz, M. H. Kaplan, R. C. Gallo, and M. Popovic.** 1986. The role of mononuclear phagocytes in HTLV-III/LAV infection. Science **233:**215–219.
9. **Glas, J., H. P. Torok, C. Simperl, A. Konig, K. Martin, F. Schmidt, M. Schaefer, U. Schiemann, and C. Folwaczny.** 2003. The Delta 32 mutation of the chemokine-receptor 5 gene neither is correlated with chronic hepatitis C nor does it predict response to therapy with interferon alpha and ribavirin. Clin. Immunol. **108:**46–50.
10. **Gribble, G. W.** 1975. Reactions of sodium borohydride in acidic media. Selective reduction of aldehydes with sodium triacetoborohydride. JCS Chem. Comm. **1975:**535–541.
11. **Kavlick, M. F., and H. Mitsuya.** 2001. The emergence of drug-resistant human immunodeficiency virus type 1 variants and its impact on antiretroviral therapy of human immunodeficiency virus type 1 infection, p. 279–312. *In* E. de Clerq (ed.), The art of antiretroviral therapy. American Society for Microbiology, Washington, D.C.
12. **Koh, Y., H. Nakata, K. Maeda, H. Ogata, G. Bilcer, T. Devasamudram, J. F. Kincaid, P. Boross, Y. F. Wang, Y. Tie, P. Volarath, L. Gaddis, R. W. Harrison, I. T. Weber, A. K. Ghosh, and H. Mitsuya.** 2003. Novel bis-tetrahydrofuranylurethane-containing nonpeptidic protease inhibitor (PI) UIC-94017 (TMC114) with potent activity against multi-PI-resistant human immunodeficiency virus in vitro. Antimicrob. Agents Chemother. **47:**3123–3129.
13. **Koyanagi, Y., W. A. O'Brien, J. Q. Zhao, D. W. Golde, J. C. Gasson, and I. S. Chen.** 1988. Cytokines alter production of HIV-1 from primary mononuclear phagocytes. Science **241:**1673–1675.
14. **Lee, B., M. Sharron, C. Blanpain, B. J. Doranz, J. Vakili, P. Setoh, E. Berg, G. Liu, H. R. Guy, S. R. Durell, M. Parmentier, C. N. Chang, K. Price, M. Tsang, and R. W. Doms.** 1999. Epitope mapping of CCR5 reveals multiple conformational states and distinct but overlapping structures involved in chemokine and coreceptor function. J. Biol. Chem. **274:**9617–9626.
15. **Liu, R., W. A. Paxton, S. Choe, D. Ceradini, S. R. Martin, R. Horuk, M. E. MacDonald, H. Stuhlmann, R. A. Koup, and N. R. Landau.** 1996. Homozygous defect in HIV-1 coreceptor accounts for resistance of some multiply-exposed individuals to HIV-1 infection. Cell **86:**367–377.
16. **Lusso, P., F. Cocchi, C. Balotta, P. D. Markham, A. Louie, P. Farci, R. Pal, R. C. Gallo, and M. S. Reitz, Jr.** 1995. Growth of macrophage-tropic and primary human immunodeficiency virus type 1 (HIV-1) isolates in a unique $CD4^+$ T-cell clone (PM1): failure to downregulate CD4 and to interfere with cell-line-tropic HIV-1. J. Virol. **69:**3712–3720.
17. **Maeda, K., K. Yoshimura, S. Shibayama, H. Habashita, H. Tada, K. Sagawa, T. Miyakawa, M. Aoki, D. Fukushima, and H. Mitsuya.** 2001. Novel low molecular weight spirodiketopiperazine derivatives potently inhibit R5 HIV-1 infection through their antagonistic effects on CCR5. J. Biol. Chem. **276:**35194–35200.
18. **Maeda, Y., M. Foda, S. Matsushita, and S. Harada.** 2000. Involvement of both the V2 and V3 regions of the CCR5-tropic human immunodeficiency virus type 1 envelope in reduced sensitivity to macrophage inflammatory protein 1alpha. J. Virol. **74:**1787–1793.
19. **Marozsan, A. J., V. S. Torre, M. Johnson, S. C. Ball, J. V. Cross, D. J. Templeton, M. E. Quinones-Mateu, R. E. Offord, and E. J. Arts.** 2001. Mechanisms involved in stimulation of human immunodeficiency virus type 1 replication by aminooxypentane RANTES. J. Virol. **75:**8624–8638.
20. **Mitsuya, H., and J. Erickson.** 1999. Discovery and development of antiretroviral therapeutics for HIV infection, p. 751–780. *In* T. C. Merigan, J. G. Bartlet, and D. Bolognesi (ed.), Textbook of AIDS medicine. Williams & Wilkins, Baltimore, Md.
21. **Miyakawa, T., K. Obaru, K. Maeda, S. Harada, and H. Mitsuya.** 2002. Identification of amino acid residues critical for LD78beta, a variant of human macrophage inflammatory protein-1alpha, binding to CCR5 and inhibition of R5 human immunodeficiency virus type 1 replication. J. Biol. Chem. **277:**4649–4655.
22. **Moriuchi, H., M. Moriuchi, and A. S. Fauci.** 1998. Factors secreted by human T lymphotropic virus type I (HTLV-I)-infected cells can enhance or inhibit replication of HIV-1 in HTLV-I-uninfected cells: implications for *in vivo* coinfection with HTLV-I and HIV-1. J. Exp. Med. **187:**1689–1697.
23. **O'Brien, S. J., and J. P. Moore.** 2000. The effect of genetic variation in chemokines and their receptors on HIV transmission and progression to AIDS. Immunol. Rev. **177:**99–111.
24. **Olson, W. C., G. E. Rabut, K. A. Nagashima, D. N. Tran, D. J. Anselma, S. P. Monard, J. P. Segal, D. A. Thompson, F. Kajumo, Y. Guo, J. P. Moore, P. J. Maddon, and T. Dragic.** 1999. Differential inhibition of human immunodeficiency virus type 1 fusion, gp120 binding, and CC-chemokine activity by monoclonal antibodies to CCR5. J. Virol. **73:**4145–4155.
25. **Samson, M., F. Libert, B. J. Doranz, J. Rucker, C. Liesnard, C. M. Farber, S. Saragosti, C. Lapoumeroulie, J. Cognaux, C. Forceille, G. Muyldermans, C. Verhofstede, G. Burtonboy, M. Georges, T. Imai, S. Rana, Y. Yi, R. J. Smyth, R. G. Collman, R. W. Doms, G. Vassart, and M. Parmentier.** 1996. Resistance to HIV-1 infection in caucasian individuals bearing mutant alleles of the CCR-5 chemokine receptor gene. Nature **382:**722–725.
26. **Shirasaka, T., M. F. Kavlick, T. Ueno, W. Y. Gao, E. Kojima, M. L. Alcaide, S. Chokekijchai, B. M. Roy, E. Arnold, R. Yarchoan, and H. Mitsuya.** 1995. Emergence of human immunodeficiency virus type 1 variants with resistance to multiple dideoxynucleosides in patients receiving therapy with dideoxynucleosides. Proc. Natl. Acad. Sci. USA **92:**2398–2402.
27. **Siliciano, J. D., J. Kajdas, D. Finzi, T. C. Quinn, K. Chadwick, J. B. Margolick, C. Kovacs, S. J. Gange, and R. F. Siliciano.** 2003. Long term follow-up studies confirm the stability of the latent reservoir for HIV 1 in resting $CD4^+$ T cells. Nat. Med. **9:**727–728.
28. **Strizki, J. M., S. Xu, N. E. Wagner, L. Wojcik, J. Liu, Y. Hou, M. Endres, A. Palani, S. Shapiro, J. W. Clader, W. J. Greenlee, J. R. Tagat, S. McCombie, K. Cox, A. B. Fawzi, C. C. Chou, C. Pugliese Sivo, L. Davies, M. E. Moreno, D. D. Ho, A. Trkola, C. A. Stoddart, J. P. Moore, G. R. Reyes, and B. M. Baroudy.** 2001. SCH-C (SCH 351125), an orally bioavailable, small molecule antagonist of the chemokine receptor CCR5, is a potent inhibitor of HIV-1 infection in vitro and in vivo. Proc. Natl. Acad. Sci. USA **98:**12718–12723.
29. **Thelen, M.** 2001. Dancing to the tune of chemokines. Nat. Immunol. **2:**129–134.
30. **Tsamis, F., S. Gavrilov, F. Kajumo, C. Seibert, S. Kuhmann, T. Ketas, A. Trkola, A. Palani, J. W. Clader, J. R. Tagat, S. McCombie, B. Baroudy, J. P. Moore, T. P. Sakmar, and T. Dragic.** 2003. Analysis of the mechanism by which the small-molecule CCR5 antagonists SCH 351125 and SCH-350581 inhibit human immunodeficiency virus type 1 entry. J. Virol. **77:**5201–5208.
31. **Trkola, A., S. E. Kuhmann, J. M. Strizki, E. Maxwell, T. Ketas, T. Morgan, P. Pugach, S. Xu, L. Wojcik, J. Tagat, A. Palani, S. Shapiro, J. W. Clader, S. McCombie, G. R. Reyes, B. M. Baroudy, and J. P. Moore.** 2002. HIV-1 escape from a small molecule, CCR5-specific entry inhibitor does not involve CXCR4 use. Proc. Natl. Acad. Sci. USA **99:**395–400.
32. **Veazey, R. S., P. J. Klasse, T. J. Ketas, J. D. Reeves, M. Piatak, Jr., K. Kunstman, S. E. Kuhmann, P. A. Marx, J. D. Lifson, J. Dufour, M. Mefford, I. Pandrea, S. M. Wolinsky, R. W. Doms, J. A. DeMartino, S. J. Siciliano, K. Lyons, M. S. Springer, and J. P. Moore.** 2003. Use of a small molecule CCR5 inhibitor in macaques to treat simian immunodeficiency virus infection or prevent simian-human immunodeficiency virus infection. J. Exp. Med. **198:**1551–1562.
33. **Vodicka, M. A., W. C. Goh, L. I. Wu, M. E. Rogel, S. R. Bartz, V. L. Schweickart, C. J. Raport, and M. Emerman.** 1997. Indicator cell lines for detection of primary strains of human and simian immunodeficiency viruses. Virology **233:**193–198.
34. **Westervelt, P., H. E. Gendelman, and L. Ratner.** 1991. Identification of a determinant within the human immunodeficiency virus 1 surface envelope glycoprotein critical for productive infection of primary monocytes. Proc. Natl. Acad. Sci. USA **88:**3097–3101.
35. **Woitas, R. P., G. Ahlenstiel, A. Iwan, J. K. Rockstroh, H. H. Brackmann, B. Kupfer, B. Matz, R. Offergeld, T. Sauerbruch, and U. Spengler.** 2002. Frequency of the HIV-protective CC chemokine receptor 5-Delta32/Delta32 genotype is increased in hepatitis C. Gastroenterology **122:**1721–1728.
36. **Yoshimura, K., R. Kato, K. Yusa, M. F. Kavlick, V. Maroun, A. Nguyen, T. Mimoto, T. Ueno, M. Shintani, J. Falloon, H. Masur, H. Hayashi, J. Erickson, and H. Mitsuya.** 1999. JE-2147: a dipeptide protease inhibitor (PI) that potently inhibits multi-PI-resistant HIV-1. Proc. Natl. Acad. Sci. USA **96:**8675–8680.

JOURNAL OF VIROLOGY, Oct. 2004, p. 11352–11359 Vol. 78, No. 20
0022-538X/04/$08.00+0 DOI: 10.1128/JVI.78.20.11352–11359.2004

A Lentiviral cDNA Library Employing Lambda Recombination Used To Clone an Inhibitor of Human Immunodeficiency Virus Type 1-Induced Cell Death

Yuji Kawano,[1] Takeshi Yoshida,[1,2] Kuniko Hieda,[1,2] Jun Aoki,[1,2] Hiroyuki Miyoshi,[3] and Yoshio Koyanagi[2]*

Department of Virology, Tohoku University Graduate School of Medicine, Sendai,[1] Laboratory of Viral Pathogenesis, Institute for Virus Research, Kyoto University, Kyoto,[2] and BioResource Center, RIKEN Tsukuba Institute, Tsukuba,[3] Japan

Received 17 November 2003/Accepted 27 May 2004

Expression cloning technology of cDNAs is a suitable tool for identifying novel functional properties of genes. Here, we generated a lentiviral cDNA library-expressing system for human T cells based on a site-specific recombination system of phage lambda for transferring cDNA libraries with a minimum loss of its complexity. The library-transduced $CD4^+$ T cells were challenged with wild-type human immunodeficiency virus type 1 (HIV-1), and the cells that acquired resistance to HIV-1-induced cytopathic effect (CPE) were selected. From these cells, CD14 was isolated and proved to inhibit the entry of HIV-1 and the HIV-1-induced CPE. This cloning system allows rapid identification of genes encoding novel properties in human T cells and probably other mammalian cells.

A number of screening systems from genetic libraries have been developed to identify novel functional properties of the genes. A successful screening with mammalian cells is dependent on the efficiency of the transduction system into the appropriate target cells. A plasmid-based expression system has been generally used (1, 2, 17). However, this system has a limit due to the inefficient transfection into particular cells, such as nonadherent cells. In addition, the introduced genes are expressed only transiently. Therefore, it is desirable to develop a new technology that can efficiently achieve long-lasting expression of genetic information in the nonadherent cells, especially human lymphocytes. Retrovirus vectors appear to overcome these limits (16). Retrovirus infects a wide range of mammalian cell types, including lymphocytes, with a high efficiency. The library-inserted retrovirus vector can integrate into the host's chromosome and is expressed permanently. These properties have been utilized for a gene delivery system for lymphocytes (16). However, the prototype murine leukemia virus-based retrovirus vector infects only dividing cells (12) and, less efficiently, human T cells. Thus, the target cells for screening are limited. Recently, a human immunodeficiency virus (HIV)-based lentivirus vector was developed (12), and such vectors are beginning to be used in many applications (4, 7, 10, 11).

In this report, we describe the development of a lentiviral cDNA library expression system applicable for human T cells. The results showed significant utility of the system to clone genes through a high-throughput screening procedure. This system allowed us to identify genes that render cells resistant to HIV-induced cell death. Our lentivirus system is promising, as it can be applied to many library screening systems, and should accelerate the discovery of novel properties of the genes in many other cells including neurons and hematopoietic stem cells.

* Corresponding author. Mailing address: Laboratory of Viral Pathogenesis, Institute for Virus Research, Kyoto University, 53 Shougoinkawahara cho, Sakyou-ku, Kyoto 606-8507, Japan. Phone: 81-22-717-8210. Fax: 81-75-751-4812. E-mail: ykoyanag@virus.kyoto-u.ac.jp.

MATERIALS AND METHODS

Cells. Human 293T were maintained in Dulbecco's modified Eagle medium containing 10% fetal calf serum, and MT-4 cells were maintained in RPMI 1640 containing 10% fetal calf serum.

Gateway-compatible lentiviral cDNA library system and HIV-1 challenge. A Gateway-compatible lentivirus vector DNA (pYK005C) was constructed through the insertion of a Gateway cloning system reading frame cassette (Invitrogen, Carlsbad, Calif.) into the EcoRI site of the multiple cloning sites (MCS) in the HIV-1-based vector DNA, pCSII-elongation factor 1α promoter (EF)-MCS-internal ribosome entry site (IRES)-humanized *Renilla* green fluorescent protein (hrGFP) (9). For the generation of the entry cDNA library, 10 ng (≈1.5×10^9 copies) of the original cDNA library generated from human peripheral blood leukocytes (Invitrogen) was amplified by PCR with the following primers: 5′-GGGGACAAGTTTGTACAAAAAAGCAGGCT-3′ and 5′-GGGGACCACTTTGTACAAGAAAGCTGGGT-3′ (underlined nucleotides are the *att*B [B1 and B2] sequences in the forward and reverse primers, respectively). The cycling conditions were 94°C for 2 min, 94°C for 15 s, 55°C for 30 s, and 68°C for 5 min for 15 cycles and 68°C for 10 min. PCR products and pDONR201 DNA (Invitrogen) were incubated with BP Clonase enzyme mix (Invitrogen) for 16 h at 25°C by using the procedure recommended by the manufacturer, and the resulting recombinant molecules were transformed in DH5α. The transformants were selected with kanamycin (50 μg/ml), and the resultant entry cDNA library was prepared from pools of transformants. For the generation of the vector cDNA library, 300 ng of the entry cDNA library and 360 ng of pYK005C vector DNA, which is linearized by digestion with EcoRI, were incubated with LR Clonase enzyme mix (Invitrogen) for 19 h at 25°C. All resulting recombinant molecules were transformed in DH5α and selected on plates containing ampicillin (50 μg/ml). The resultant vector cDNA library was prepared from pools of transformants. For preparation of cDNA-expressing lentivirus vector, a vesicular stomatitis virus (VSV)-pseudotyped lentivirus vector was generated via calcium phosphate-mediated transfection of 293T cells as described before (9). Briefly, 1.2×10^7 cells were divided onto six TC dishes (100 × 20; Nunc, Roskilde, Denmark) 24 h before transfection. Seventeen micrograms of Vector cDNA library DNA, 12 μg of HIV Gag-Pol-expressing vector (pMDLg/pRRE), 5 μg of VSV-G protein-expressing vector (pMD-G), and 5 μg of HIV Rev-expressing vector (pRSV-Rev) per dish were cotransfected, then 48 h later, the culture supernatants were collected, and virus particles were concentrated 30-fold by centrifugation at 6,000 × *g* for 16 h. The concentrated viruses were titrated with MT-4 cells. For transduction of the cDNA library into T cells and HIV type 1 (HIV-1) challenge, 1.2×10^7 MT-4 cells were infected with 8×10^6 infectious doses of the

viral cDNA library. Three days later, the cells were challenged with HIV-1_{NL4-3} at a multiplicity of infection (MOI) of 0.05. For recovery of the cDNA sublibrary from surviving cells, MT-4 cells that survived HIV-1 challenge were collected and genomic DNA was extracted. The cDNAs from the surviving cells were amplified by PCR with primers that were used to amplify the original cDNA library as described above. This cDNA sublibrary was transferred to the pDONR201 vector by a BP reaction, and the resultant entry cDNA sublibrary was transferred to pYK005C lentivirus vector DNA by an LR reaction as described above. The viral cDNA sublibrary was prepared via transfection of 293T cells and used for the second round of screening.

Flow cytometric analysis. Two-color flow cytometric analysis was performed. Briefly, cells were stained with the optimal concentration of antibody for 30 min at 4°C and then washed. Phycoerythrin-conjugated anti-human CD4 and CD14 (eBioscience, San Diego, Calif.) and anti-mouse *H-2K*^{k} (Cedarlane, Ontario, Canada) were used. HIV-1 expression was examined with an anti-HIV-1 human serum followed by staining with biotin-conjugated anti-human IgG (Vector Laboratories, Burlingame, Calif.) and streptavidin-conjugated peridinin chlorophyll protein (BD Biosciences, San Jose, Calif.). The data were collected by FACScan (BD PharMingen, San Diego, Calif.) and analyzed with WinMDI software.

Sequence analysis. cDNA cloned into the pDONR201 vector was analyzed with the 5′-TCGCGTTAACGCTAGCATGGATCTC-3′ primer. The data were collected with the ABI 377 autosequencer. The sequence data were compared with the DNA database at the National Center for Biotechnology Information by using BLAST search.

Determination of individual cDNA length. The original cDNA library, the entry cDNA library, and the vector cDNA library were applied to *Escherichia coli* competent cells, and the cells were spread onto Luria-Bertani plates to develop bacterial colonies. cDNA fragments were amplified by PCR from these bacterial colonies containing each cDNA fragment. The PCR products were subjected to agarose gel electrophoresis and visualized with ethidium bromide. The migration distance of each cDNA fragment was compared with a DNA size marker. MT-4 cells transduced with the viral cDNA library were cloned by the limiting dilution method. cDNA fragments were amplified by PCR from the cloned cells. The length of each cDNA was determined as described above.

CD14 cDNA transduction and HIV-1 infection. A CD14 cDNA-expressing construct was made through the insertion of the Gateway cloning system reading frame cassette (Invitrogen) into the EcoRI site of the pIRES-hrGFP vector (Stratagene, San Diego, Calif.), and then a CD14 cDNA fragment was isolated from the library by an LR reaction. CD4$^+$CCR5$^+$ HeLa cells (6) were transfected by Lipofectamine 2000 (Invitrogen) with the CD14-expressing construct or empty vector (pIRES-hrGFP) as a control, and then 48 h later, the cells were infected with HIV-1_{NL4-3} at an MOI of 2. Cells were harvested 2, 12, 24, and 48 h after HIV-1 infection, and DNA was extracted as described before (20). For CD14 stable transduction, an *H-2K*^{k}-expressing lentivirus vector, which was constructed by replacing the mutant *Renilla reniformis* hrGFP sequence in the Gateway-compatible lentivirus vector DNA (pYK005C) with the *H-2K*^{k} sequence, was used. MT-4 or CD4$^+$ CCR5$^+$ HeLa cells were infected with either the CD14-expressing or control lentivirus vector at an MOI of 1, and then 2 days later, the cells were challenged with HIV-1_{NL4-3} at an MOI of 0.05. Cell killing activity was measured by trypan blue staining, and virus production in the culture supernatant was monitored by enzyme-linked immunosorbent assay (ZeptoMetrix Corp., Buffalo, N.Y.) for the HIV-1 p24^{gag} antigen.

Real-time PCR assay. For the detection and quantification of individual forms of HIV-1 DNA, strong-stop (early reverse transcript), full-length/1-LTR circle (late reverse transcript), 2-LTR circle, and integrated forms, a real-time PCR assay was used as described previously (20). PCR was performed with an ABI PRISM 7700 sequence detection system (PE Applied Biosystems, Foster City, Calif.) and *Taq*Man universal PCR master mix (PE Applied Biosystems).

Statistical analysis. The Mann-Whitney U test was used to determine statistical significance, and P values of <0.05 were considered significant.

RESULTS

Transfer of a cDNA library from a cloning expression vector into a donor vector. Since some leukocytes would produce antiviral proteins, we started to isolate anti-HIV genes from a cDNA library generated from human peripheral blood leukocytes. Since a plasmid-based expression vector via transfection cannot be used for efficient and stable transduction into T cells, a lentiviral cDNA library-expressing system was used to introduce genes into human T cells. In this system, we used a recombination-cloning system referred to as Gateway (22). The Gateway system, which has been used to transfer individual genes (22), is based on the recombination system of the phage lambda that mediates integration and excision of the phage DNA into and from the *E. coli* genome, respectively. The integration involves recombination of the *att*P sites (P1 and P2) of the phage DNA within the *att*B sites (B1 and B2) located in the bacterial genome (BP reaction) and generates an integrated phage genome flanked by *att*L (L1 and L2) and *att*R (R1 and R2) sites. The next excision results in these *att*L and *att*R sites back to the *att*P and *att*B sites (LR reaction). First of all, the cDNA library fragments inserted between bacterial genome-derived B1 and B2 sites of the pCMV-SPORT6 cloning expression vector, referred to as the original cDNA library, were amplified by PCR. The PCR product was purified and incubated with a donor vector containing an insertion of the P1 and P2 sites, pDONR201, in the presence of BP clonase enzyme mix, which consists of a mixture of the phage protein integrase (Int) and the bacterial protein integration host factor. The BP clonase recombines the B1 and P1 sites as well as the B2 and P2 sites (BP reaction), and as a result, the cDNA library fragments were placed between derivatives of the L1 and L2 sites. The cDNA library-inserted pDONR201 was referred to as the entry cDNA library. Although a similar number of independent cDNA-carrying clones was obtained after this transfer, the mean size of the cDNA was clearly reduced from 1.75 ± 0.82 kb to 1.34 ± 0.66 kb (± standard deviations [SD]; $n = 60$; $P < 0.05$, Mann-Whitney U test), as shown in Table 1. Generally, the short DNA fragment tends to be more efficiently amplified during PCR. This property may account for the reduction of the cDNA size. However, omission of the PCR resulted in an obvious reduction of the number of independent cDNA-carrying clones by about 1/25. Thus, the PCR amplification before the BP reaction was indispensable.

TABLE 1. Quality of cDNA libraries

cDNA library	No. of primary clones	Mean insert size ± SD (kb)[a]
Original	1×10^7	1.75 ± 0.82
Entry	1.5×10^7	1.34 ± 0.66
Vector	8×10^7	1.26 ± 0.65
Viral	ND[b]	0.71 ± 0.54

[a] Mean insert size was determined by electrophoresis of PCR fragments from 60 bacterial colonies (original, entry, and vector libraries) or from 190 cDNA clones in viral cDNA library-infected cells.
[b] ND, not done.

Transfer of the entry cDNA library into a lentivirus vector. Next, the entry cDNA library was incubated with a lentivirus vector DNA that had derivatives of the R1 and R2 sites in the presence of the LR clonase enzyme mix that consists of a mixture of the phage protein excisionase (Xis), Int, and integration host factor. The LR clonase recombines the L1 and R1 sites as well as the L2 and R2 sites (LR reaction), and DNA fragments between L1 and L2 were placed between the B1 and B2 sites, respectively. Although *cis*-acting sequences derived from the lentivirus vector may interfere with wild-type HIV-1 replication, a part of the vector with a deletion of the U3 region (self-inactivating vectors) was not responsive to the interference (3). Therefore, a self-inactivating vector was used in this study. The cDNA library transferred into the lentivirus

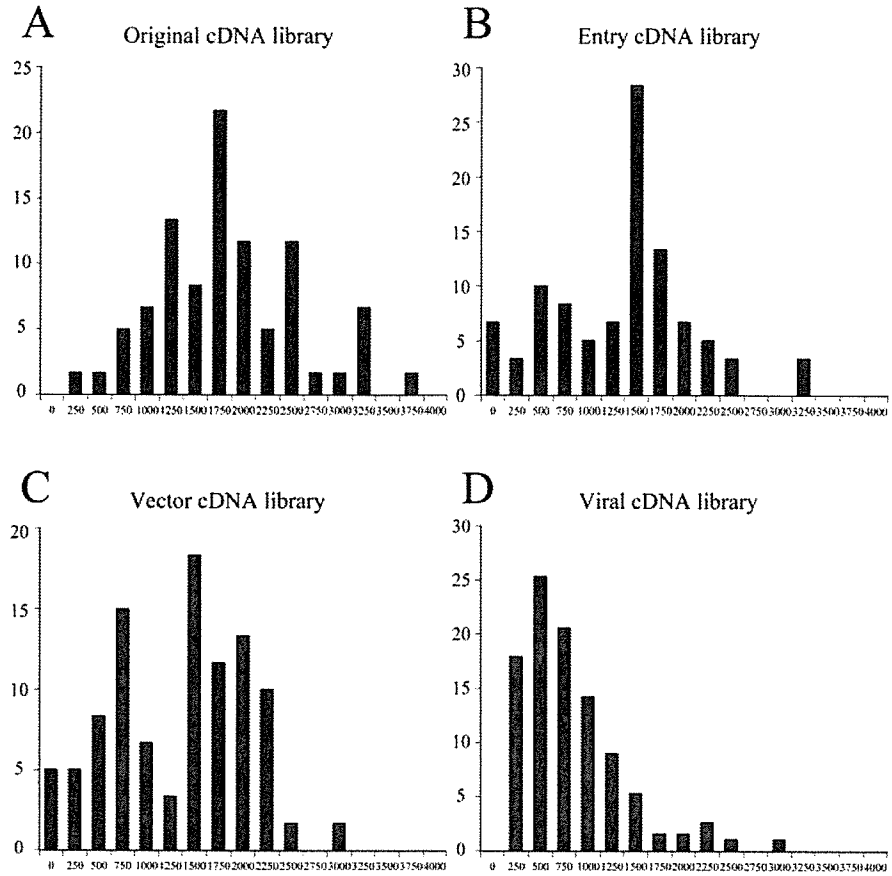

FIG. 1. Histogram analysis of lengths of individual cDNA fragments in each library. The lengths of cDNA fragments were determined as described in Materials and Methods and are plotted in 250-bp increments on the *x* axes. Percentages of individual clones are indicated on the *y* axes.

vector DNA was referred to as the vector cDNA library. Because this lentivirus vector expresses the cDNA library, under the control of elongation factor α promoter, along with GFP expression from a single bicistronic transcript, cDNA library-transduced cells are easily identified by flow cytometry or fluorescent microscopy. After this transfer, no reductions in the number or cDNA size of independent cDNA-carrying clones were observed (Table 1; Fig. 1), suggesting that the library inserted between the L1 and L2 sites would be transferred into another vector without significant loss of library complexity.

Generation of a cDNA library-expressing lentivirus vector. Next we prepared a cDNA library-expressing lentivirus vector, referred to as the viral cDNA library, via cotransfection of 293T cells with vector cDNA library DNA, a VSV-G protein expression DNA, an HIV Gag-Pol expression DNA, and an HIV Rev expression DNA. The infectious titer was approximately 4×10^6/ml, measured by using a human $CD4^+$-T-cell line, MT-4 cells. On the other hand, the infectious titer of the parental lentivirus vector with no cDNA inserted, CSII-EF-MCS-IRES-hrGFP (9), was 10 to 100 times higher than that of the viral cDNA library (data not shown). The average size of cDNA fragments in the transduced cells was 0.7 kb, which was shorter than that of cDNA fragments in the vector cDNA library, suggesting that the smaller cDNAs were enriched during lentivirus preparation and its infection into cells (Table 1; Fig. 1). To overcome this problem, size fractionation to enrich long cDNA fragments should be performed in future experiments. Nevertheless, some transduced cDNAs were more than 2,000 bp (Fig. 1), suggesting that this vector system can transduce more than 2,000-bp cDNA fragments.

Cloning of genes that prevent cells from HIV-1-induced cell death. Figure 2 shows an outline of the selection system used to isolate anti-HIV genes from the library used in this study. Twelve million MT-4 cells were infected with the viral cDNA library at an MOI of approximately 0.68. The total number of cDNA-transduced cells was estimated to be around 8×10^6, which was slightly smaller than the number of independent clones of the original cDNA library. Three days after cDNA transduction, the cells were challenged with HIV-1_{NL4-3} at an MOI of 0.05. About 30 days after HIV-1 challenge, when nontransduced culture cells had been completely killed, surviving cells, all of which were continuously growing, and GFP^+ cells were collected and cellular DNA was extracted. The cDNA fragments were recovered by PCR with B1 and B2 primers and transferred into pDONR201 vector DNA through the BP reaction. Then the cDNA sublibrary-expressing lentivirus was generated. After subsequent screening through transduction of the cDNA sublibrary in MT-4 cells and subsequent HIV-1 challenge, more than 25 independent cDNA clones were isolated, which were confirmed in further experiments to

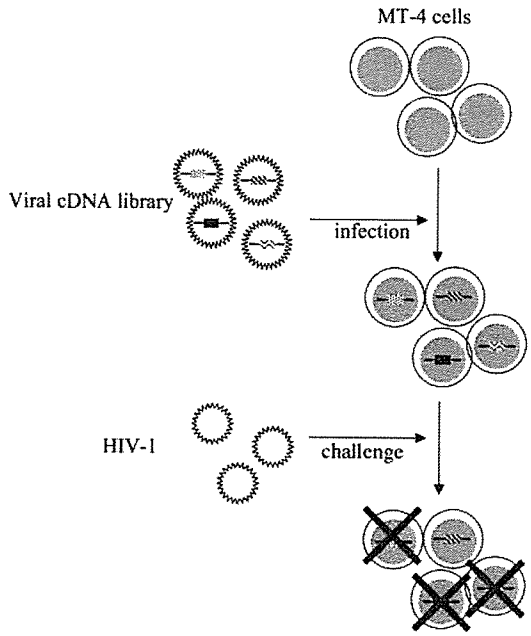

FIG. 2. Scheme for strategy used to select genes that arm cells with resistance to HIV-induced CPE. MT-4 cells were infected with the viral cDNA library and then challenged with HIV-1_{NL4-3}, which is highly cytopathic to MT-4 cells. If the introduced gene has anti-CPE, the cell will survive in the presence of HIV-1.

confer the cytopathic effect (CPE)-free phenotype in the transduced cells after HIV-1 challenge. Sequence analysis revealed that these clones contained full-length CD14 cDNA, and their sequence was identical to that of BC010507 in the GenBank database. Flow cytometric analysis showed that the anti-CD14 antibody reacted only with the cDNA clone-transduced $CD4^+$ cell population (Fig. 3A) identified by GFP expression (Fig. 3B and C).

To verify the effect of CD14 on HIV-1 infection, we independently prepared three cell lines: MT-4 cells transduced with a lentivirus vector that express CD14 along with GFP from a single bicistronic transcript, MT-4 cells transduced with an $H\text{-}2K^k$-expressing lentivirus vector, and nontransduced MT-4 cells. Flow cytometric analysis confirmed that all GFP-expressing cells simultaneously and persistently expressed CD14 on the cell surface (Fig. 4A). The three cell lines were mixed, and the cultures were challenged with wild-type HIV-1. Before HIV-1 infection, the mixed culture consisted of three cell populations: GFP^+ $H\text{-}2K^{k-}$, GFP^- $H\text{-}2K^{k+}$, and GFP^- $H\text{-}2K^{k-}$ cells (Fig. 4B). Only the GFP^+ $H\text{-}2K^{k-}$ population survived after HIV-1 infection (Fig. 4C). In contrast, the proportion of the three cell types was consistently maintained in HIV-1-uninfected cultures (Fig. 4D). Trypan blue staining confirmed that all dead cells were GFP^- and all GFP^+ cells were alive (Fig. 4E, F, and G). A subsequent flow cytometric analysis of cells stained by anti-HIV-1 human sera indicated that the CD14-transduced MT-4 cells also expressed HIV-1 antigen (Fig. 4H and I). When the CD14 gene was transduced into human $CD4^+$ $CCR5^+$ HeLa cells, these cells were also susceptible to HIV-1 infection but resistant to HIV-1-induced cell death (data not shown). To reveal the mechanism of how CD14 is blocking the HIV-1-induced cell death, the effect of CD14 for HIV-1 replication was examined. The surface expression of neither CD4 nor CXCR4 was altered in CD14-transduced MT-4 cells (data not shown). On the other hand, the HIV-1 replication in CD14-transduced cells determined by production of $p24^{gag}$ antigen in culture supernatant was significantly lower than that in control vector-transduced cells (Fig. 5A and B). To determine the level at which HIV-1 replication is inhibited by CD14, we used a real-time PCR assay to detect individual forms of viral cDNA at various times after HIV-1 infection. Since the preceding transduction with an HIV-1-based lentiviral vector will hamper the real-time PCR assay to measure the level of newly synthesized HIV-1 cDNA only originated from subsequent wild-type HIV-1 infection, a CD14-expressing plasmid DNA or control vector DNA was

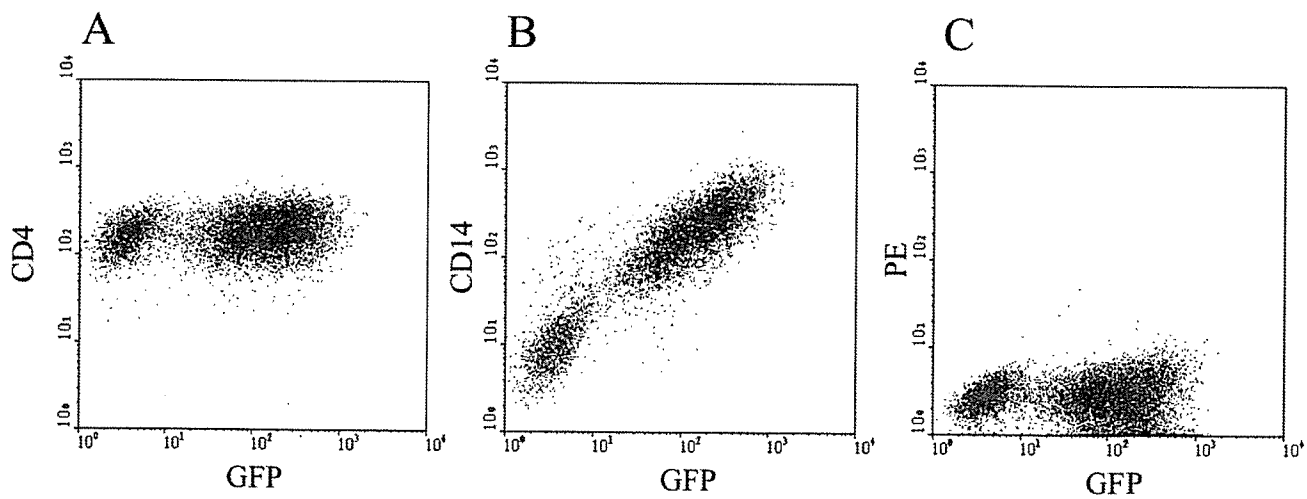

FIG. 3. Characterization of a cDNA clone that confers T-cell resistance to HIV-1-induced CPE. Cells transduced with the CD14-carrying vector isolated from this viral cDNA library were stained with anti-CD4 antibody (A), anti-CD14 antibody (B), or isotype-matched control antibody (C) and analyzed by flow cytometry. The results shown are data from one flow cytometry experiment, which is representative of three independent experiments. PE, phycoerythrin.

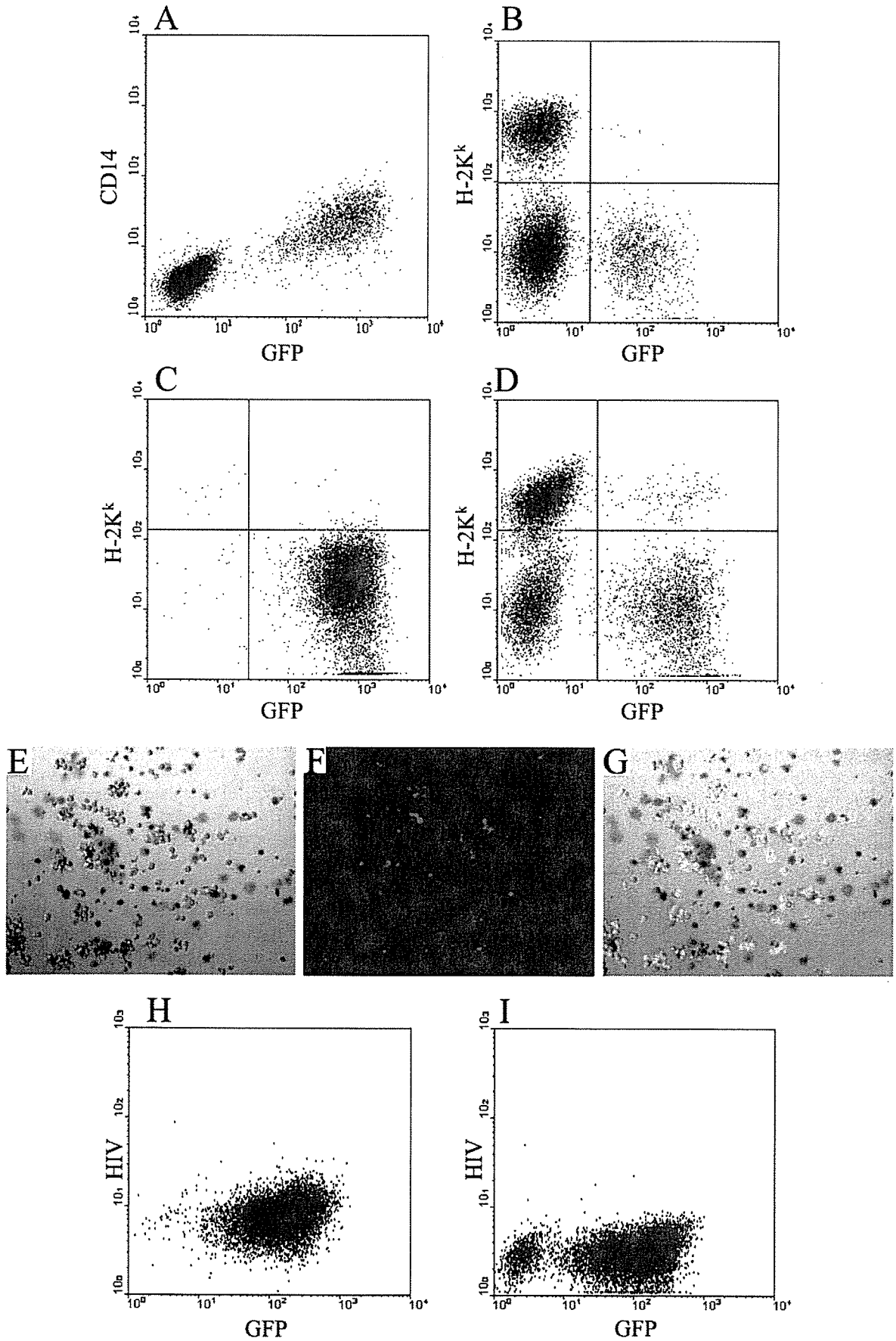
A
CD14
GFP
B
H-2K^k
GFP
C
H-2K^k
GFP
D
H-2K^k
GFP
E
F
G
H
HIV
GFP
I
HIV
GFP

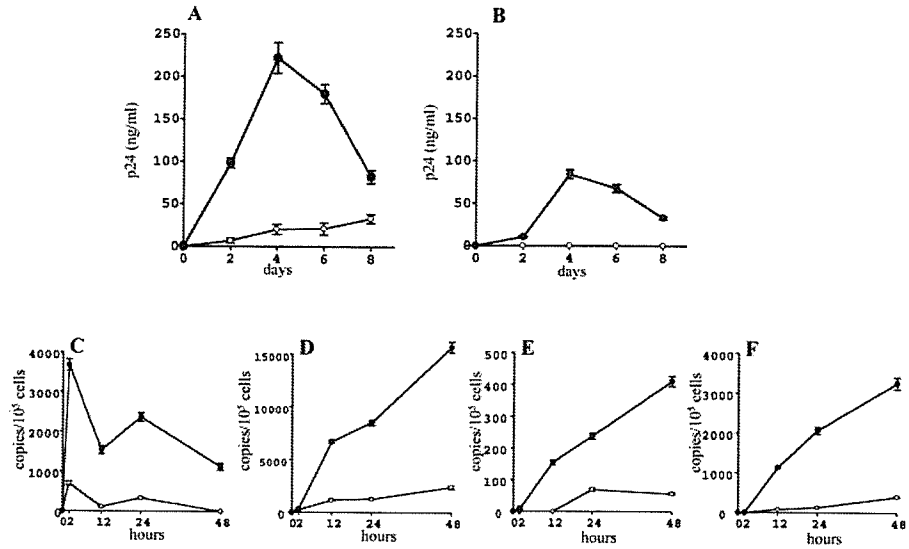

FIG. 5. Inhibition of HIV-1 replication in CD14-transduced cells. HIV-1 replication was evaluated by production of $p24^{gag}$ antigen in the culture supernatant of CD14- or empty vector-transduced MT-4 (A) or $CD4^+$ $CCR5^+$ HeLa cells (B) with a lentivirus vector expressing CD14 and *H-2K*^{k} or *H-2K*^{k} alone, respectively. To determine the level of HIV-1 entry efficiency, CD14- or empty vector-transfected $CD4^+$ $CCR5^+$ HeLa cells were challenged with DNase-treated $HIV\text{-}1_{NL4\text{-}3}$. Target cell DNA was isolated at the indicated time and used to detect early reverse transcripts (C), late reverse transcripts (D), 2-LTR circle (E), and the integrated form (F). Data are the means ± SD from duplicate experiments. The levels of the $p24^{gag}$ antigen or HIV-1 DNA in the CD14-transduced cultures were significantly lower than those of the empty vector-transduced cultures ($P < 0.05$, Mann-Whitney U test). Lines with open circles, CD14 vector; lines with filled circles, empty vector.

transfected into $CD4^+$ $CCR5^+$ HeLa cells. More than 70% of cells were confirmed to express the CD14 molecule on the cell surface determined by flow cytometry 2 days after transfection, and then the culture was infected with $HIV\text{-}1_{NL4\text{-}3}$ (X4 virus). The levels of early reverse transcripts, late reverse transcripts, 2-LTR circle, and the integrated form were significantly lower in the CD14-expressing culture than in control culture (Fig. 5C, D, E, and F). However, when $CD4^+$ $CCR5^+$ HeLa cells were infected with $HIV\text{-}1_{NL4\text{-}3}$ and then 2 days later transfected with the CD14-expressing DNA, the HIV-1 release, determined by production of the $p24^{gag}$ antigen in the culture supernatant, was similar in both the CD14-transfected and control cultures (data not shown). These data indicate that CD14 appears to partially inhibit the entry step in HIV-1 replication and provide the HIV CPE-free phenotype.

DISCUSSION

In this study, we established a lentivirus vector system to transduce a cDNA library into human T cells and successfully isolated an anti-CPE gene against HIV-1 infection. A wide variety of expression systems in mammalian cells have been developed, for example, plasmid-based, virus-based, and transposon-based systems. Among them, retrovirus-based and lentivirus-based expression systems can stably transduce genes into human T cells and are, furthermore, efficient enough to screen 10^7 genes. Recently, van Maanen et al. (21) reported the potential use of a lentivirus vector in an expression cloning system. However, the vast majority of cDNA libraries have not been yet constructed on lentivirus vectors. If a cDNA library is efficiently constructed on a lentivirus vector, this vector system will be strongly powerful to isolate genes and accelerate functional genomics. Hence, we used a site-specific recombination system, Gateway, for transferring a cDNA library from a transient expression vector to a lentivirus vector. The major advantage of this transfer system is that we can apply the system to many already established libraries. For instance, a cDNA library amplified in phage can be transferred to a mammalian expression vector including the lentivirus vector without significant loss of its complexity. Many reports have suggested that this technology allows for easy transfer of individual cDNA fragments, and this technology has become a powerful tool for a high-throughput screening system in functional genomics (8, 14, 18, 19). In this study, we used a premade cDNA library in a transient expression vector that cannot be efficiently intro-

FIG. 4. Resistance to HIV-1-induced cell death in CD14-transduced T cells. (A) Flow cytometric analysis of MT-4 cells infected with a CD14- and GFP-expressing lentivirus vector was performed. These cells (GFP^+ *H-2K*$^{k-}$) were mixed with cells infected with a lentivirus vector expressing *H-2K*^{k} alone (GFP^- *H-2K*$^{k+}$) and uninfected cells (GFP^- *H-2K*$^{k-}$) and then challenged with $HIV\text{-}1_{NL4\text{-}3}$. Flow cytometric analysis of the mixed culture is shown before HIV-1 challenge (B), 8 days after HIV-1 challenge (C), and 8 days after mock infection (D). Trypan blue staining (E) and fluorescent microscopic examination (F) were performed 3 days after HIV-1 challenge. A merged image of panels E and F is shown in panel G. Magnification, ×200. Flow cytometric analysis of the HIV-1-challenged culture 10 days after infection (H) or of an uninfected culture (I) was performed by staining with anti-HIV human serum. The results shown are data from one experiment, which is representative of three independent experiments.

duced into T cells. Here, we successfully transferred the cDNA library to a lentivirus vector and found that CD14 can confer resistance to HIV-induced cell death in the transduced cells. This observation suggests that the transferred libraries can still be applied for a functional screening system. Because the vector has also been used to transduce genes into nondividing cells such as neurons (11, 12), muscles (7), and hematopoietic stem cells (4), our lentivirus-based system can be applied to expression cloning systems that use such cells.

However, there is a need to improve our library transfer system. Some degree of loss in library complexity was noted. In our experiment, some of the cDNAs, especially long cDNA fragments, appeared to be lost during two steps: PCR amplification and lentivirus vector production and/or infection. This problem would be solved when the long cDNA fragments are enriched before the BP reaction and a genetic library is directly generated on a donor vector for the LR reaction. We think the latter strategy is useful because, if a library is constructed on a donor vector, the library can be transferred to various expression vector systems, which include not only the lentivirus vector but also other traditional vector systems, by only the LR reaction. As shown in Table 1, we did not observe the loss of library complexity during the LR reaction in our experiment. To overcome the loss of parts of the long cDNA fragments during production of lentivirus vector and/or infection, shorter parent lentiviral vector DNAs should be used in future experiments. In the present study, we used a GFP-expressing lentivirus vector DNA (CSII-EF-MCS-IRES-hrGFP). To obtain long cDNA inserts in the lentiviral vector, there is probably a need to delete some parts of the fragment within the vector DNA, such as IRES-hrGFP.

It was reported that the lentivirus (derived from HIV-1) vector-transduced T cells are less susceptible to wild-type HIV-1 infection than nontransduced T cells (3). The transcripts transduced by the vector appears to compete efficiently for encapsidation, resulting in inhibition of its infectivity, probably because *cis*-acting sequences in the lentivirus vector are responsive to the regulatory protein of wild-type HIV-1. However, the inhibitory effect was completely eliminated in a self-inactivating vector (3). Thus, we used a self-inactivating vector, and we could not actually find any differences in its HIV-1 replication ability between the transduced and nontransduced cells (data not shown).

In the present study, we used a cDNA library as a functional genetic element. In the future, we will be able to choose different genetic libraries, such as ribozyme (8) and peptide libraries (23, 25). The ribozyme library can be efficiently expressed under the control of an RNA polymerase III-dependent promoter (8). When constructing a lentivirus vector containing such a library, the Gateway-based transfer system will be useful. Moreover, since the length of such a library is more homogeneous and shorter than a conventional cDNA library, the lentivirus vector system will be able to more potently deliver a ribozyme library than a cDNA library.

CD14 is known as a coreceptor molecule for lipopolysaccharide (LPS) (24) and is expressed on the surface of myeloid cells via a glycosylphosphatidyl inositol tail. LPS binds to a serum protein, LPS-binding protein (15), and associates with CD14. Subsequently, LPS stimulates Toll-like receptor 4 (13) and activates signaling pathways, mainly the nuclear factor-κB (NF-κB) pathway. HIV-1 also preferentially infects macrophages that express CD14. It is known that macrophages are one of the major target cells for HIV infection, and they behave as cellular reservoirs of virions in HIV-infected patients, probably because the cells are relatively resistant to HIV-induced CPE (5). Although the mechanisms of the low susceptibility of macrophages to HIV-1-induced cell death are poorly understood at present, some explanations may be brought up from the resistance of CD14-transduced cells to HIV-1-induced cell death. One explanation is that overexpression of CD14 can trigger cell survival signals such as NF-κB or induce antiapoptotic genes. Another explanation is that CD14 can reduce the cytotoxicity of HIV-1 infection in T cells through a partial inhibition of HIV-1 replication. In fact, CD14 overexpression resulted in an inhibition of the entry step on HIV-1 replication, as shown in Fig. 5. A determination of the exact mechanisms of CD14 function in HIV-infected cells should enhance our understanding of the cellular events during HIV-induced cell death, which results in immune destruction in HIV-infected individuals.

In conclusion, application of the Gateway system to a genetic library transfer system will allow the use of the lentivirus vector system as a powerful tool for the study of functional genomics of mammalian cells.

ACKNOWLEDGMENTS

We thank I. Verma for providing several reagents used in our study.

This work was supported by a Grant-in-Aid for Scientific Research on Priority Areas from the Ministry of Education, Culture, Sports, Sciences, and Technology of Japan; by grants for Research on HIV-AIDS and Health Science from the Ministry of Health, Labor, and Welfare of Japan. Y. Koyanagi was also supported by a grant from the Naito Foundation.

REFERENCES

1. **Aruffo, A., and B. Seed.** 1987. Molecular cloning of a CD28 cDNA by a high-efficiency COS cell expression system. Proc. Natl. Acad. Sci. USA **84:** 8573–8577.
2. **Aruffo, A., and B. Seed.** 1987. Molecular cloning of two CD7 (T-cell leukemia antigen) cDNAs by a COS cell expression system. EMBO J. **6:**3313–3316.
3. **Bukovsky, A. A., J. P. Song, and L. Naldini.** 1999. Interaction of human immunodeficiency virus-derived vectors with wild-type virus in transduced cells. J. Virol. **73:**7087–7092.
4. **Case, S. S., M. A. Price, C. T. Jordan, X. J. Yu, L. Wang, G. Bauer, D. L. Haas, D. Xu, R. Stripecke, L. Naldini, D. B. Kohn, and G. M. Crooks.** 1999. Stable transduction of quiescent $CD34^+CD38^-$ human hematopoietic cells by HIV-1-based lentiviral vectors. Proc. Natl. Acad. Sci. USA **96:**2988–2993.
5. **Gartner, S., P. Markovits, D. M. Markovitz, M. H. Kaplan, R. C. Gallo, and M. Popovic.** 1986. The role of mononuclear phagocytes in HTLV-III/LAV infection. Science **233:**215–219.
6. **Hachiya, A., S. Aizawa-Matsuoka, M. Tanaka, Y. Takahashi, S. Ida, H. Gatanaga, Y. Hirabayashi, A. Kojima, M. Tatsumi, and S. Oka.** 2001. Rapid and simple phenotypic assay for drug susceptibility of human immunodeficiency virus type 1 using CCR5-expressing HeLa/$CD4^+$ cell clone 1–10 (MAGIC-5). Antimicrob. Agents Chemother. **45:**495–501.
7. **Kafri, T., U. Blomer, D. A. Peterson, F. H. Gage, and I. M. Verma.** 1997. Sustained expression of genes delivered directly into liver and muscle by lentiviral vectors. Nat. Genet. **17:**314–317.
8. **Ko, M. S. H.** 2001. Embryogenomics: developmental biology meets genomics. Trends Biotechnol. **19:**511–518.
9. **Kuwata, H., Y. Watanabe, H. Miyoshi, M. Yamamoto, T. Kaisho, K. Takeda, and S. Akira.** 2003. IL-10-inducible Bcl-3 negatively regulates LPS-induced TNF-α production in macrophages. Blood **102:**4123–4129.
10. **Miyoshi, H., K. A. Smith, D. E. Mosier, I. M. Verma, and B. E. Torbett.** 1999. Transduction of human $CD34^+$ cells that mediate long-term engraftment of NOD/SCID mice by HIV vectors. Science **283:**682–686.
11. **Naldini, L., U. Blomer, F. H. Gage, D. Trono, and I. M. Verma.** 1996. Efficient transfer, integration, and sustained long-term expression of the transgene in adult rat brains injected with a lentiviral vector. Proc. Natl. Acad. Sci. USA **93:**11382–11388.

12. **Naldini, L., U. Blomer, P. Gallay, D. Ory, R. Mulligan, F. H. Gage, I. M. Verma, and D. Trono.** 1996. In vivo gene delivery and stable transduction of nondividing cells by a lentiviral vector. Science **272:**263–267.
13. **Poltorak, A., X. He, I. Smirnova, M.-Y. Liu, C. V. Huffel, X. Du, D. Birdwell, E. Alejos, M. Silva, C. Galanos, M. Freudenberg, P. Ricciardi-Castagnoli, B. Layton, and B. Beutler.** 1998. Defective LPS signaling in C3H/HeJ and C57BL/10ScCr mice: mutations in Tlr4 gene. Science **282:**2085–2088.
14. **Reboul, J., P. Vaglio, N. Tzellas, N. Thierry-Mieg, T. Moore, C. Jackson, T. Shin-i, Y. Kohara, D. Thierry-Mieg, J. Thierry-Mieg, H. Lee, J. Hitti, L. Doucette-Stamm, J. L. Hartley, G. F. Temple, M. A. Brasch, J. Vandenhaute, P. E. Lamesch, D. E. Hill, and M. Vidal.** 2001. Open-reading-frame sequence tags (OSTs) support the existence of at least 17,300 genes in C. elegans. Nat. Genet. **27:**332–336.
15. **Schumann, R. R., S. R. Leong, G. W. Flaggs, P. W. Gray, S. D. Wright, J. C. Mathison, P. S. Tobias, and R. J. Ulevitch.** 1990. Structure and function of lipopolysaccharide binding protein. Science **249:**1429–1431.
16. **Seed, B.** 1995. Developments in expression cloning. Curr. Opin. Biotechnol. **6:**567–573.
17. **Seed, B., and A. Aruffo.** 1987. Molecular cloning of the CD2 antigen, the T-cell erythrocyte receptor, by a rapid immunoselection procedure. Proc. Natl. Acad. Sci. USA **84:**3365–3369.
18. **Shevchenko, Y., G. G. Bouffard, Y. S. Butterfield, R. W. Blakesley, J. L. Hartley, A. C. Young, M. A. Marra, S. J. Jones, J. W. Touchman, and E. D. Green.** 2002. Systematic sequencing of cDNA clones using the transposon Tn5. Nucleic Acids Res. **30:**2469–2477.
19. **Simpson, J. C., V. E. Neubrand, S. Wiemann, and R. Pepperkok.** 2001. Illuminating the human genome. Histochem. Cell Biol. **115:**23–29.
20. **Suzuki, Y., N. Misawa, C. Sato, H. Ebina, T. Masuda, N. Yamamoto, and Y. Koyanagi.** 2003. Quantitative analysis of human immunodeficiency virus type 1 DNA dynamics by real-time PCR: integration efficiency in stimulated and unstimulated peripheral blood mononuclear cells. Virus Genes **27:**177–188.
21. **van Maanen, M., J. K. Tidwell, L. A. Donehower, and R. E. Sutton.** 2003. Development of an HIV-based cDNA expression cloning system. Mol. Ther. **8:**167–173.
22. **Walhout, A. J. N. M., R. Sordella, X. Lu, J. L. Hartley, G. F. Temple, M. A. Brasch, N. Thierry-Mieg, and M. Vidal.** 2000. Protein interaction mapping in C. elegans using proteins involved in vulval development. Science **287:**116–122.
23. **Welch, P. J., E. G. Marcusson, Q.-X. Li, C. Beger, M. Kruger, C. Zhou, M. Leavitt, F. Wong-Staal, and J. R. Barber.** 2000. Identification and validation of a gene involved in anchorage-independent cell growth control using a library of randomized hairpin ribozymes. Genomics **66:**274–283.
24. **Wright, S. D., R. A. Ramos, P. S. Tobias, R. J. Ulevitch, and J. C. Mathison.** 1990. CD14, a receptor for complexes of lipopolysaccharide (LPS) and LPS binding protein. Science **249:**1431–1433.
25. **Xu, X., C. Leo, Y. Jang, E. Chan, D. Padilla, B. C. Huang, T. Lin, T. Gururaja, Y. Hitoshi, J. B. Lorens, D. C. Anderson, B. Sikic, Y. Luo, D. G. Payan, and G. P. Nolan.** 2001. Dominant effector genetics in mammalian cells. Nat. Genet. **27:**23–29.

JOURNAL OF VIROLOGY, Feb. 2005, p. 2087–2096
0022-538X/05/$08.00+0 doi:10.1128/JVI.79.4.2087–2096.2005

Vol. 79, No. 4

Potent Anti-R5 Human Immunodeficiency Virus Type 1 Effects of a CCR5 Antagonist, AK602/ONO4128/GW873140, in a Novel Human Peripheral Blood Mononuclear Cell Nonobese Diabetic-SCID, Interleukin-2 Receptor γ-Chain-Knocked-Out AIDS Mouse Model

Hirotomo Nakata,[1] Kenji Maeda,[1] Toshikazu Miyakawa,[1] Shiro Shibayama,[2] Masayoshi Matsuo,[2] Yoshikazu Takaoka,[2] Mamoru Ito,[3] Yoshio Koyanagi,[4]† and Hiroaki Mitsuya[1,5]*

Department of Infectious Diseases, Kumamoto University Graduate School of Medicine, Kumamoto,[1] Ono Pharmaceutical Co. Ltd., Osaka,[2] Central Institute for Experimental Animals, Kawasaki,[3] Department of Virology, Tohoku University Graduate School of Medicine, Sendai,[4] Japan, and Experimental Retrovirology Section, HIV and AIDS Malignancy Branch, National Cancer Institute, Bethesda, Maryland[5]

Received 27 May 2004/Accepted 1 October 2004

We established human peripheral blood mononuclear cell (PBMC)-transplanted R5 human immunodeficiency virus type 1 isolate JR-FL (HIV-1_{JR-FL})-infected, nonobese diabetic-SCID, interleukin 2 receptor γ-chain-knocked-out (NOG) mice, in which massive and systemic HIV-1 infection occurred. The susceptibility of the implanted PBMC to the infectivity and cytopathic effect of R5 HIV-1 appeared to stem from hyperactivation of the PBMC, which rapidly proliferated and expressed high levels of CCR5. When a novel spirodiketopiperazine-containing CCR5 inhibitor, AK602/ONO4128/GW873140 (molecular weight, 614), was administered to the NOG mice 1 day after R5 HIV-1 inoculation, the replication and cytopathic effects of R5 HIV-1 were significantly suppressed. In saline-treated mice ($n = 7$), the mean human $CD4^+/CD8^+$ cell ratio was 0.1 on day 16 after inoculation, while levels in mice ($n = 8$) administered AK602 had a mean value of 0.92, comparable to levels in uninfected mice ($n = 7$). The mean number of HIV-RNA copies in plasma in saline-treated mice were $\sim 10^6$/ml on day 16, while levels in AK602-treated mice were 1.27×10^3/ml ($P = 0.001$). AK602 also significantly suppressed the number of proviral DNA copies and serum p24 levels ($P = 0.001$). These data suggest that the present NOG mouse system should serve as a small-animal AIDS model and warrant that AK602 be further developed as a potential therapeutic for HIV-1 infection.

Highly active antiretroviral therapy has brought about a major impact on the AIDS epidemics in the industrially advanced nations (5, 22). However, eradication of human immunodeficiency virus type 1 (HIV-1) is thought to be currently impossible, due in part to the viral reservoirs remaining in blood and infected tissues (6). The limitation of antiviral therapy of AIDS is exacerbated by complicated regimens, the development of drug-resistant HIV-1 variants (11), and a number of inherent adverse effects (2, 31). Hence, the identification of new antiretroviral drugs that have unique mechanisms of action and produce no or minimal adverse effects remains an important therapeutic objective. In regard to development of potential anti-HIV therapies or vaccines, experimental animal models for AIDS which allow the determination of the possible efficacy of antiviral agents or vaccines have been sought since severe combined immunodeficiency (SCID) mice engrafted with human fetal thymus, liver, or peripheral blood mononuclear cells (PBMC) were first exploited to examine antiretroviral agents (19, 25). However, a number of mouse models have suffered from false-positive and false-negative results in detecting or quantifying HIV-1 infection and replication and have required a large number of samples and mice for testing (25, 29).

In the present work, we established human PBMC-transplanted R5 HIV-1_{JR-FL}-infected, nonobese diabetic (NOD)-SCID, interleukin 2 receptor γ (IL-2Rγ)-chain-knocked-out (NOG) mice, in which massive and systemic HIV-1 infection occurs, human $CD4^+/CD8^+$ cell ratios significantly decrease, and high levels of R5 HIV-1 viremia reaching as high as 10^6 copies/ml are achieved. Furthermore, we demonstrated that this unprecedented susceptibility of the implanted human PBMC to the infectivity and cytopathic effects of R5 HIV-1 infection stems from hyperactivation of the PBMC. Here, we also report a novel small nonpeptide CCR5 antagonist, AK602/ONO4128/GW873140, which exerts potent anti-HIV-1 activity in vitro against laboratory and clinical strains of HIV-1, including highly multidrug-resistant (MDR) variants.

* Corresponding author. Mailing address: Department of Infectious Diseases, Kumamoto University Graduate School of Medicine, 1-1-1 Honjo, Kumamoto 860-8556, Japan. Phone: 81-96-373-5156. Fax: 81-96-363-5265. E-mail: hmitsuya@helix.nih.gov.

† Present address: Laboratory of Viral Pathogenesis, Institute for Virus Research, Kyoto University, Kyoto 606-8507, Japan.

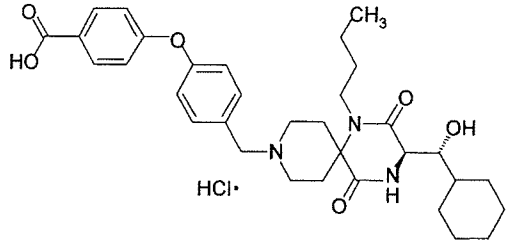

FIG. 1. Structure of AK602.

MATERIALS AND METHODS

Transplantation of human PBMC in NOG mice. NOD-SCID (NOG) mice (10, 33) were maintained in the Central Institute for Experimental Animals (Kawasaki, Japan). Mice were 4 to 6 weeks old at the time of transfer of human PBMC. The human PBMC-transplanted NOG (hu-PBMC-NOG) mice were generated by methods previously described (23, 24). Briefly, PBMC (10^7) were freshly prepared from heparinized blood of a single healthy HIV-1-seronegative donor by Ficoll-Hypaque density gradient centrifugation, resuspended in RPMI 1640-based culture medium (0.5 ml), and infused intraperitoneally to each mouse. The experimental protocol was approved by the Ethics Review Committees for Animal Experimentation of the participating institutions.

Assay for proliferation and CCR5 expression of transplanted human PBMC recovered from hu-PBMC-NOG mice. Freshly isolated human PBMC (2×10^7 cells/ml) were incubated in phosphate-buffered saline (PBS) containing 10 μM 5-carboxyfluorescein diacetate succinimidyl ester (CFSE; Molecular Probes, Eugene, Oreg.) for 15 min at 37°C for CFSE labeling as previously described by Lyons (16), washed, and resuspended in RPMI 1640. One part of the labeled PBMC preparation was intraperitoneally injected (10^7 PBMC) to each NOG mouse, and human PBMC were recovered from peritoneal lavages and spleen. The other part of the preparation was immediately stimulated with 10 μg of phytohemagglutinin (PHA)/ml, cultured, and harvested. PBMC samples thus obtained were labeled with phycoerythrin (PE)-conjugated anti-CCR5 monoclonal antibody 3A9 or peridinin chlorophyll protein-conjugated anti-HLA-DR antibody (BD Pharmingen, San Diego, Calif.) and subjected to flow cytometric analysis with a Becton Dickinson FACscan cytometer; the data were analyzed by Cell Quest software (Becton Dickinson, Franklin Lakes, N.J.). A quantitative fluorescence-activated cell sorting (FACS) assay that relies on a series of precalibrated beads that bind to a fixed number of mouse immunoglobulin G molecules (Quantum Simply Cellular Kit; Sigma, Saint Louis, Mo.) to determine the absolute number of CCR5s on the cell surface was also conducted according to the manufacturer's instructions (15).

Cells and viruses. The HeLa-CD4-LTR-β-gal indicator cell line expressing human CCR5 ($CCR5^+$ MAGI) (18), a kind gift from Yosuke Maeda, was used for the present study. 293T cells (a human embryonic kidney cell line) were cultured in Dulbecco's modified Eagle medium supplemented with 10% fetal calf serum (FCS) and antibiotics and used for transfection of DNA plasmid containing the R5 HIV-$1_{JR\text{-}FL}$ genome (13). PBMC isolated from HIV-1-seronegative individuals were cultured with 10% FCS and antibiotics with 10 μg of PHA/ml for 3 days prior to anti-HIV-1 activity assay in vitro (PHA-PBMC). A panel of HIV-1 strains was employed for the drug susceptibility attempt: HIV-$1_{Ba\text{-}L}$ (7), HIV-$1_{JR\text{-}FL}$ (13), HIV-$1_{NL4\text{-}3}$ (32), a wild-type HIV-1_{MOKW} isolated from a drug-naive AIDS patient (17), and MDR primary HIV-1 (HIV-1_{MDR}) strain (HIV-1_{JSL} and HIV-1_{MM}) (35). All primary HIV-1 strains were passaged once or twice in PHA-PBMC cultures and the culture supernatants were stored at −80°C until use. Antiviral assays using PHA-PBMC were conducted as previously reported (12, 17, 35).

Antiviral agents and assay for inhibition of R5 HIV-1 infectivity and replication. A series of different spirodiketopiperazine (SDP) derivatives were newly designed, synthesized, and tested for their activity against in vitro infectivity and replication of R5 HIV-1 as previously described (17). AK602 was chosen for this study based on its CCR5-specific, potent activity against R5 HIV-1. A method for the synthesis of AK602 will be published elsewhere. The structure of AK602 is illustrated in Fig. 1. An approved drug for therapy for HIV-1 infection, 2′,3′-dideoxyinosine (ddI) (20, 21), was kindly provided by Ajinomoto Co., Inc, Tokyo, Japan. TAK779 and SCH-C were synthesized according to previously published data (1, 30). The MAGI assay using $CCR5^+$ MAGI cells was conducted as previously described (17) with minor modifications. Briefly, $CCR5^+$ MAGI cells were seeded in 96-well, flat-bottomed microculture plates (10^4 cells/well) for 24 h, exposed to 0.1 or 1 μM AK602 for 30 min, washed three times, exposed to R5 HIV-1 (100 50% tissue culture infectious doses) at various time points after AK602 removal, and cultured in Dulbecco's modified Eagle medium containing 15% FCS for 48 h. Following the removal of supernatants and lysis of the cells with PBS (100 μl) containing 1% Triton X-100, a solution (100 μl) containing 10 mM chlorophenol red-β-D-galactopyranoside, 2 mM $MgCl_2$, and 0.1 M KH_2PO_4 was added to each well; the mixture was incubated at room temperature in the dark for 30 min; and the optical density (wavelength, 570 nm) was measured with a microplate reader (*V*max, Molecular Devices, Sunnyvale, Calif). All assays were performed in triplicate.

Pharmacokinetic analysis of AK602 in hu-PBMC-NOG mice. Pharmacokinetic analysis of AK602 in hu-PBMC-NOG mice was performed as previously described (28). In brief, plasma samples were collected periodically over 12 h, following a single AK602 administration at a dose of 60 mg/kg of body weight dissolved in 400 μl of 4% hydroxypropyl-β cyclodextrin (HPBC). Each plasma sample (150 μl) was centrifuged at 3,000 rpm for 10 min, and the supernatant was vacuum concentrated and injected into the high-performance liquid chromatography (HPLC) system. The eluent was monitored at 255 nm of UV, and the AK602 concentration in plasma was determined.

Determination of amounts of AK602 persistently bound to CCR5 in hu-PBMC-NOG mice. Blood samples were collected from the tail vein of each hu-PBMC-NOG mouse at various time points following a single intraperitoneal administration of AK602 at a dose of 60 mg/kg. PBMC were isolated by density gradient centrifugation and stained with fluorescein isothiocyanate-conjugated monoclonal antibody 45531 (R&D Systems, Minneapolis, Minn.) specific for the C-terminal half of the second extracellular loop (ECL2B) of CCR5 (15) known to be competitively replaced by SDP derivatives (17) or with PE-conjugated monoclonal antibody 3A9, which binds to the N-terminus extracellular domain of CCR5 (17). PBMC were then subjected to FACS analysis.

Treatment of R5 HIV-1-infected hu-PBMC-NOG mice with anti-HIV-1 agents. Sixteen days after PBMC infusion, the mice were bled from the tail vein, and three-color flow cytometric analysis was performed to confirm positive engraftment of human HLA, CD4, and CD8 antigens on the cells recovered. HIV-$1_{JR\text{-}FL}$ (2,000 50% tissue culture infectious doses) was intraperitoneally inoculated to each mouse in which PBMC engraftment was confirmed. Twenty-four hours after the R5 HIV-1 inoculation, administration of AK602 (120 mg in 4% HPBC/kg/day, twice a day), ddI (50 mg in 4% HPBC/kg/day, twice a day), or saline was implemented and continued by day 16. On days 5 and 9 after the R5 HIV-1 inoculation, blood samples were collected from mouse tail veins for immunologic and virological monitoring (see below). On day 16, blood samples were collected by cardiocentesis, and the mice were sacrificed. The experimental protocol for the treatment is illustrated in Fig. 2.

Immunologic and virological monitoring. Human PBMC recovered from mice were subjected to immunologic and virological monitoring as previously described (23, 24). The $CD4^+/CD8^+$ cell ratios were determined by FACS analysis with PE-conjugated mouse anti-CD4 and peridinin chlorophyll protein-conjugated mouse anti-CD8 (BD Pharmingen) monoclonal antibodies. Determination of HIV-1 DNA copy numbers in recovered human PBMC was performed by real-time PCR assay with Taqman Master mixture (PE Biosystems) and HIV long terminal repeat-specific primers M667 (5′-GGC TAA CTA GGG AAC CCA CTG-3′) and AA55 (5′-CTG CTA GAG ATT TTC CAC ACT GAC-3′). HIV-1-specific products were quantified with the ABI 7700 detection system (Applied Biosystems, Foster City, Calif.), and cell numbers were determined with the RAG-1 gene. The numbers of $CD4^+$ cells were calculated based on the percentage of $CD4^+$ values obtained from the FACS analysis of each test PBMC sample, and R5 HIV-1 proviral DNA copy numbers were expressed as copy numbers per 10^5 $CD4^+$ cells. In some experiments, $CD4^+$ and $CD4^-$ cells were separated before real-time PCR assay with the rapid immunomagnetic CD4-positive cell isolation kit (Dynabeads M-450 CD4; Dynal Biotech, Inc., Lake

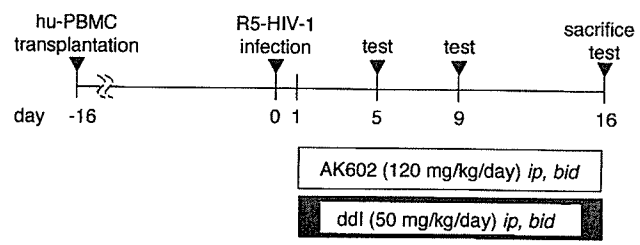

FIG. 2. Protocol for drug administration and immunological and virologic monitoring.

Success, N.Y.). The amounts of p24 antigen in murine sera were determined using a fully automated chemiluminescent enzyme immunoassay system (Lumipulse F; Fujirebio, Inc., Tokyo, Japan) as previously described (12). Plasma viral load was quantified with the AMPLICOR HIV-1 monitor test kit, version 1.5 (Roche Diagnostics, Branchburg, N.J.).

Statistical analyses. Nonparametric statistical analyses were performed by using the Mann-Whitney U test (Statview, version 5.0; Abacus Concepts, Berkeley, Calif.). The difference between viremia levels in two groups of mice was determined by the Wilcoxon rank sum test. For each mouse, the value of $\log_{10}$ RNA copies was calculated, and the slope corresponding to the rate of increase per day was determined by simple linear regression for the days (5, 9, and 16) of blood collection. The resulting slopes for all mice in the untreated groups were compared to the slopes of mice in each of the other two groups.

RESULTS

Transplanted PBMC in hu-PBMC-NOG mice are intensely activated and express high levels of CCR5. When we examined the proliferation profile of PBMC stimulated with PHA in vitro by treatment with the vital dye CFSE, which allows the analysis of cell proliferation as the CFSE's fluorescence intensity is halved per each cell division, there was only a slight shift to the left in the flow cytometric profile on days 1 and 2 of culture (Fig. 3A). On day 4 of culture, a discrete shift to the left was identified, suggesting that the PHA-PBMC underwent up to four cycles of proliferation in vitro by day 4. In contrast, PBMC transplanted and recovered on day 2 had apparently undergone ~4 cycles of proliferation; by day 4, a majority of cells had undergone up to 10 cycles and beyond in proliferation (Fig. 3B). It was possible that the CFSE-negative and weakly CFSE-positive cells which accumulated on days 2 and 4 (Fig. 3B) were murine cells that engulfed and degraded CFSE. We therefore conducted experiments in which the cells with CFSE dilution were directly confirmed to be human CCR5-positive cells. As can be seen in Fig. 3C, when cells were recovered from the spleen of an NOG mouse into which CFSE-labeled PBMC had been transplanted and stained with monoclonal antibody 45531, which is specific for the C-terminal half of the second extracellular loop (ECL2B) of CCR5 (15), the majority of such human $CCR5^+$ cells proved to be CFSE negative. We also examined the levels of cellular activation by the expression of HLA-DR on cell surface. The levels of HLA-DR expression in PBMC recovered from uninfected NOG mice 3 days after transplantation were much greater than those in 3-day-cultured PBMC following PHA stimulation (Fig. 3D). The fluorescence intensity in the same donor's PHA-PBMC examined on three different occasions was 21 ± 4, while that of the PBMC recovered from mice was 91 ± 25 (Fig. 3D). When we further assessed the levels of CCR5 expression, the PBMC recovered from the mice on day 3 proved to be strongly positive for CCR5 (Fig. 3E). The CCR5-positive fraction in the PBMC recovered was 49.7%, while that in PHA-PBMC was 27.3%. The mean fluorescence intensity of the $CCR5^+$ cell population was 141, compared to the $CCR5^+$ cell population in PHA-PBMC with a mean fluorescence intensity of 51. The estimated number of CCR5 expressed on the PBMC recovered on day 3 was 25,348 (as antibody binding sites per cell) while that on PHA-PBMC on day 3 in culture was 8,981 antibody binding sites as examined by quantitative FACS assay. These data indicate that the transplanted human PBMC were intensely activated and rapidly proliferating and expressed high levels of CCR5 on their cell surfaces.

Potent activity of AK602 against R5 HIV-1 in vitro. Among SDP derivatives we designed and synthesized, AK602 was identified to be highly potent against a broad spectrum of R5 HIV-1 strains, including MDR clinical R5 HIV-1 isolates in vitro with 50% inhibitory concentration (IC_{50}) values of 0.3 to 0.6 nM, although two previously published CCR5 antagonists (TAK779 and SCH-C) were substantially less potent than AK602 (Table 1). AK602 and other CCR5 antagonists failed to inhibit the replication of an X4 HIV-1 strain, HIV-1_{NL4-3}.

Pharmacokinetics of AK602 in hu-PBMC-NOG mice. We examined the pharmacokinetics of AK602 in hu-PBMC-NOG mice by intraperitoneally administering the compound at a dose of 60 mg/kg. Plasma samples were collected periodically up to 12 h and subjected to HPLC analysis. As shown in Fig. 4A, the concentration of AK602 reached the maximal concentration immediately after intraperitoneal administration and decreased rapidly. The calculated plasma half-life in the α-phase of the concentration curve was as short as 29 min.

AK602 persists on cell surface CCR5. As shown above, the plasma half-life of AK602 turned out to be short; however, considering that AK602 possesses such a high affinity to CCR5 and potent activity against R5 HIV-1 in vitro, it was thought possible that AK602 would remain attached on cellular CCR5 for an extensive period of time and exert anti-R5 HIV-1 activity even when the compound was depleted from circulation. To examine this possibility, we used two monoclonal antibodies, 45531 and 3A9. When human PBMC were recovered from a hu-PBMC-NOG mouse 2 and 6 h after AK602 administration (60 mg/kg) and stained with 45531, AK602 proved to block the binding of 45531 to CCR5 (Fig. 4B), while AK602 failed to block 3A9 binding to CCR5 (Fig. 4C), suggesting that AK602 did not elicit CCR5 internalization or shedding at all at least for 6 h. We subsequently examined whether AK602 remained on cellular CCR5 with the 45531 monoclonal antibody. When the cells were recovered from mice 2, 6, and 14 h after the AK602 administration, the mean values of the percentage of AK602 occupancy were 85 (four mice), 54 (three mice), and 16 (three mice), respectively. It was calculated that it took about 9 h for AK602 occupancy to be reduced by 50% (Fig. 4D).

Anti-R5 HIV-1 activity of AK602 persistently seen after its removal from culture medium. In another depletion experiment, we exposed $CCR5^+$ MAGI cells to AK602 for 30 min, depleted the compound from the culture by thorough washing, incubated the cells for various lengths of time, exposed the cells to HIV-1_{Ba-L}, further cultured the cells for 48 h, and determined whether HIV-1_{Ba-L} infection was blocked by AK602 exposure (Fig. 4E). When the $CCR5^+$ MAGI cells were exposed to 0.1 and 1 μM AK602 and exposed to HIV-1_{Ba-L} immediately afterward, the values for protection were 68 and 85%, respectively. When the cells were exposed to HIV-1_{Ba-L} 4 h after depletion, 49 and 72% of the cells were protected by 0.1 and 1 μM AK602. When the cells were exposed to HIV-1_{Ba-L} 12 and 24 h after depletion, 57 and 45% of the cells were seen protected by 1 μM, respectively (Fig. 4E).

Effects of AK602 on $CD4^+$ and $CD8^+$ cell counts in R5 HIV-1-infected hu-PBMC-NOG mice. PBMC were recovered from murine blood samples collected on days 5, 9, and 16 after R5 HIV-1 inoculation and subjected to flow cytometric analysis for determination of $CD4^+/CD8^+$ cell ratios. As shown in Fig. 5A, in PBMC recovered on day 16 from a representative

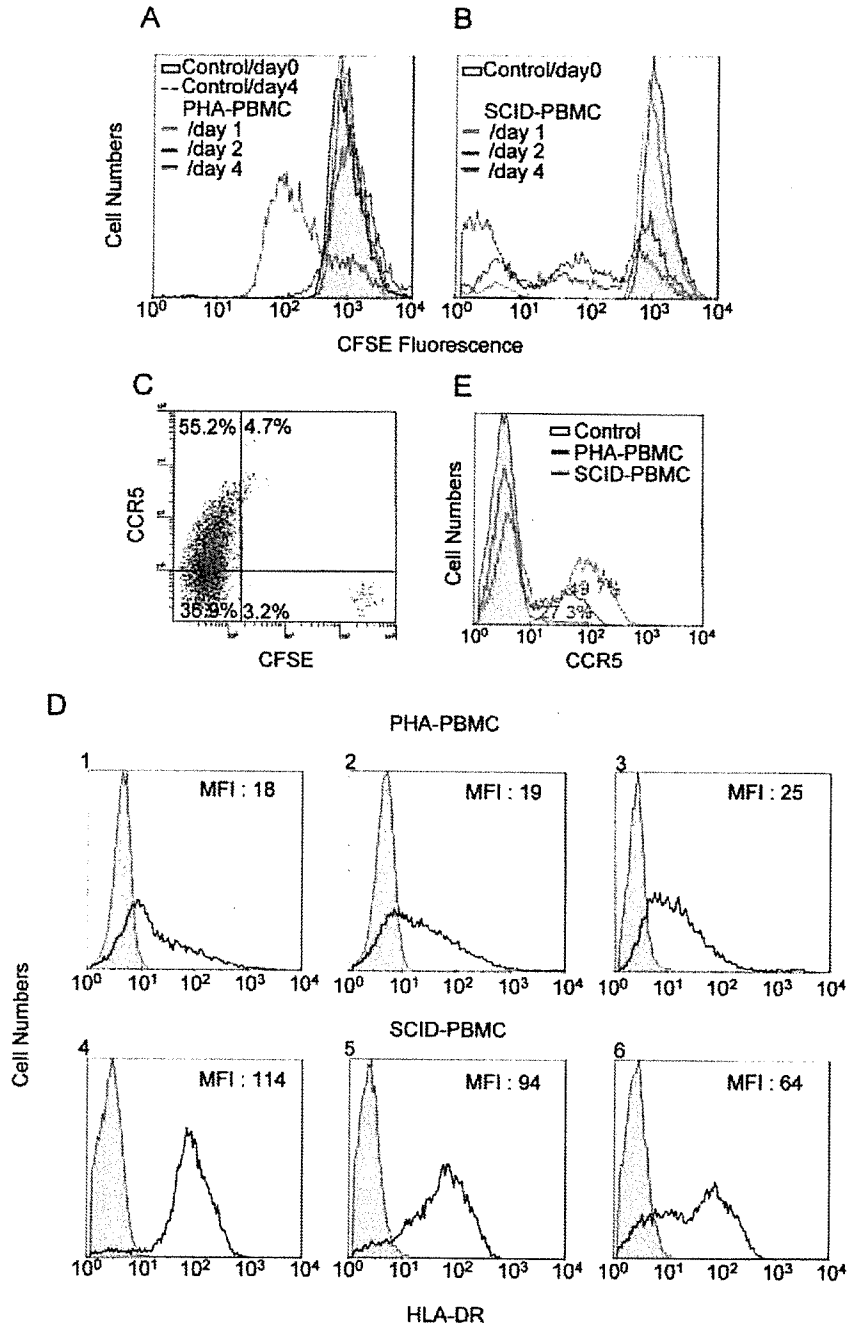

FIG. 3. Transplanted PBMC are intensely activated and express high levels of CCR5. (A and B) Proliferation profiles of PHA-PBMC and transplanted and recovered PBMC. Freshly prepared PBMC were incubated with the vital dye CFSE, and one part of such PBMC preparation was stimulated with PHA, while the other part was intraperitoneally transplanted to mice. On days 1, 2, and 4, the cells were harvested and the fluorescence intensity of CFSE was determined. Note that transplanted PBMC recovered on day 2 had undergone ~4 cycles of proliferation; by day 4, a majority of cells had undergone ~10 cycles and more of proliferation. (C) CCR5 expression level and CFSE intensity in human PBMC harvested from a spleen of hu-PBMC-NOG mouse on day 4. (D) Intense activation of PBMC after transplantation. PBMC stimulated with PHA and cultured for 4 days (panels 1 to 3) and transplanted PBMC recovered from the uninfected mice on day 4 (panels 4 to 6) were stained with an anti-HLA-DR monoclonal antibody. Note that HLA-DR expression levels in transplanted PBMC were much higher than those in PHA-PBMC. (E) CCR5 expression profiles of PHA-PBMC and transplanted PBMC. PBMC stimulated with PHA and cultured for 3 days and transplanted PBMC recovered from the uninfected mice on day 3 were stained with PE-conjugated anti-CCR5 monoclonal antibody 3A9 and subjected to flow cytometric analysis. SCID-PBMC, PBMC transplanted and recovered.

R5 HIV-1-infected, saline-treated mouse, there were only few $CD4^+$ cells (3.9% [1.4% + 2.5%]) resulting in a $CD4^+/CD8^+$ cell ratio of 0.05. However, a distinct $CD4^+$ cell population (55.1% [4.4% + 50.7%]) resulting in a $CD4^+/CD8^+$ ratio of 1.84 (Fig. 5B) was seen in PBMC recovered from an AK602-treated mouse, and the size of this $CD4^+$ cell population was comparable to that seen in a ddI-treated mouse (53.2% [3.8% + 49.4%]) and that in an uninfected mouse (48.9% [3.8% +

TABLE 1. Anti HIV-1 activity of novel SDP derivatives in PBMC[a]

Compound	IC_{50} value in p24 assay (nM)					
	HIV-1_{Ba-L} (R5)	HIV-1_{JRFL} (R5)	HIV-1_{MOKW} (R5)	HIV-1_{MM} ($R5_{MDR}$)	HIV-1_{JSL} ($R5_{MDR}$)	HIV-1_{NL4-3} (X4)
AK602	0.5 ± 0.3	0.2 ± 0.1	0.3 ± 0.2	0.7 ± 0.3	0.4 ± 0.2	>1,000
TAK779	14 ± 5	6 ± 2	9 ± 3	12 ± 4	10 ± 3	>1,000
SCH-C	3 ± 2	2 ± 1	2 ± 1.5	2.5 ± 1	2 ± 1	>1,000
ZDV	13 ± 5	7 ± 3	10 ± 6	520 ± 75	64 ± 13	9 ± 5
SQV	8 ± 3	6 ± 2	6 ± 3	212 ± 56	276 ± 44	10 ± 4

[a] IC_{50}s were determined by using PHA-PBMC isolated from three different donors, and the inhibition of p24 Gag protein production was used as an endpoint. All assays were conducted in triplicate. The results shown represent arithmetic means (±1 standard deviation) of three independently conducted assays. HIV-1_{MOKW} was isolated from a drug-naive AIDS patient, and HIV-1_{JSL} and HIV-1_{MM} were isolated from patients who received antiretroviral therapy for a long period of time and whose virus loads showed a number of RT and PR mutations. Two previously published CCR5 inhibitors, TAK779 and SCH-C, and zidovudine (ZDV) and saquinavar (SQV) were used as reference compounds.

45.1%]), resulting in the ratios of 1.43 and 1.40 (Fig. 5C and D), respectively. Figure 6A illustrates the overall profiles of $CD4^+/CD8^+$ cells ratios on day 16 in the four groups. The mean $CD4^+/CD8^+$ cell ratio in mice (n = 7) given saline was 0.1 (range, 0.06 to 0.20). In contrast, the ratios in AK602-treated mice (n = 8) were significantly higher with a mean value of 0.92 (range, 0.23 to 1.89; P = 0.001), which was comparable to that in ddI-treated mice (n = 9; mean, 1.29; range, 0.38 to 2.68; P = 0.001) and uninfected mice (n = 7; mean, 1.0; range, 0.50 to 1.49). The numbers of $CD4^+$ cells/μl

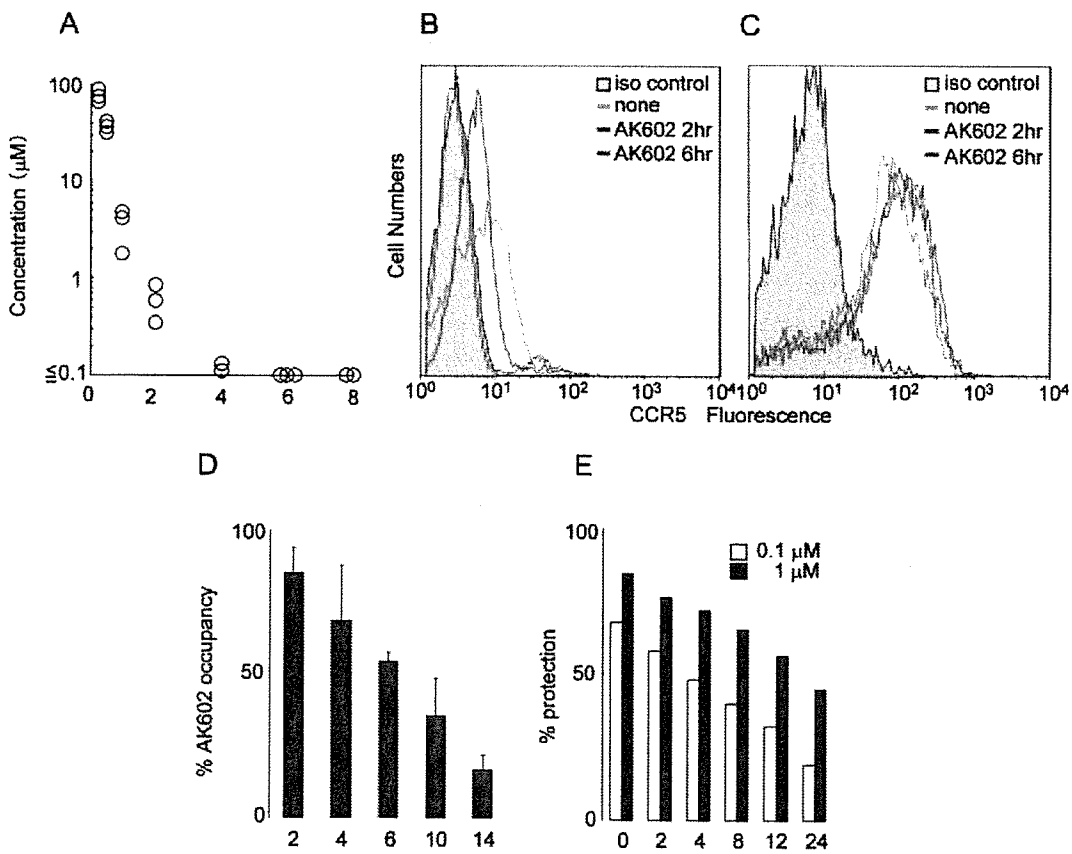

FIG. 4. Pharmacokinetics and persistence of anti-HIV-1 activity of AK602. (A) Pharmacokinetics of AK602. Each mouse was administered AK602 at a dose of 60 mg/kg, and blood samples were taken at 15, 30, 60, 120, 240, 480, and 720 min. Plasma concentrations of AK602 determined by HPLC analysis at 15, 30, 60, 120, and 240 min were 76.2, 36.1, 3.5, 0.6, and 0.13 μM, respectively. AK602 was not detected at later time points. (B and C) No CCR5 internalization or shedding was caused by AK602. Human PBMC were recovered 2 and 6 h after AK602 administration and stained with 45531 (B) or 3A9 (C). (D) Sustained AK602 occupancy on cell surfaces. At indicated periods of time after a bolus of AK-602 (60 mg/kg) was administered to hu-PBMC-NOG mice, PBMC were recovered and the percentages of AK602 occupancy on cellular CCR5 were determined with fluorescein isothiocyanate-conjugated monoclonal antibody 45531. (E) Persistence of in vitro activity of AK602 against R5 HIV-1 after AK602 depletion. $CCR5^+$ MAGI cells were exposed to 0.1 or 1 μM AK602 for 30 min and thoroughly washed to deplete AK602 from the medium. The cells were subsequently cultured for the indicated periods of time, exposed to HIV-1_{Ba-L}, and further cultured for 48 h, when the cells were harvested and lysed with Triton X-100-containing PBS. A solution containing chlorophenol red-β-D-galactopyranoside was added, the optical density was measured, and the percentage of protection was determined.

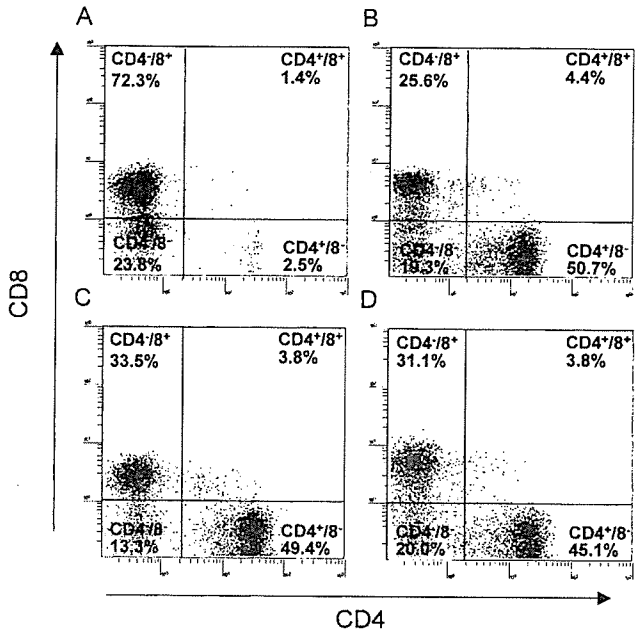

FIG. 5. Effects of AK602 on $CD4^+$ and $CD8^+$ cell counts in infected hu-PBMC-NOG mice. PBMC recovered on day 16 after R5 HIV-1 inoculation were subjected to flow cytometry. Shown are representative flow cytometric analysis profiles. Note that only 3.9% of $CD4^+$ cells were seen (A), resulting in a $CD4^+/CD8^+$ cell ratio of 0.05 in a mouse given saline, while distinct numbers of $CD4^+$ cells (55.1 and 53.2%) (B and C) were seen in AK602- and ddI-administered infected mice, resulting in $CD4^+/CD8^+$ cell ratios of 1.84 and 1.43, respectively. In an uninfected mouse (D), 48.9% of cells were positive for CD4, with a $CD4^+/CD8^+$ cell ratio of 1.40.

in saline-treated mice were significantly less than those of AK602-treated, ddI-treated, or uninfected mice (Fig. 6B).

Effects of AK602 on R5 HIV-1 proviral DNA copy numbers and serum p24 levels in R5 HIV-1-infected hu-PBMC-NOG mice. We next asked which population harbored proviral DNA in the cells recovered from R5 HIV-1-infected hu-PBMC-NOG mice, by purifying $CD4^+$ and $CD4^-$ cell populations and determining proviral DNA copy numbers in each population. As shown in Table 2, more than 99% of proviral DNA was found in $CD4^+$ cells and <0.3% of proviral DNA was detected in $CD4^-$ cells derived from saline-treated mice, indicating that R5 HIV-1 infection occurred in $CD4^+$ cells in the hu-PBMC-transplanted NOG environment. As illustrated in Fig. 6C, the mean number of R5 HIV-1 proviral DNA copies was 2.0×10^5 (range, 2.6×10^4 to 1.7×10^6) per 10^5 $CD4^+$ cells in R5 HIV-1-infected mice ($n = 7$) given saline. However, values for mice in groups given AK602 and ddI were 1.3×10^3 (range, 2.3×10^2 to 7.9×10^3; $P = 0.001$) and 1.8×10^2 (range, $<10^2$ to 7.9×10^2; $P = 0.001$), respectively.

The amounts of R5 HIV-1 p24 in serum were also found to be very high in saline-treated mice, with a mean amount of 1.1×10^5 pg/ml (range, 3.1×10^4 to 2.8×10^5 pg/ml). AK602 and ddI were found to significantly suppress the serum p24 amounts as examined on day 16 with a mean amount of 5.6×10^3 pg/ml (range, 8.1×10^2 to 2.1×10^4 pg/ml; $P = 0.001$) and 7.1×10^2 pg/ml (range, 1.3×10^2 to 1.1×10^4 pg/ml; $P = 0.001$), respectively (Fig. 6D).

AK602 suppressed R5 HIV-1 viremia in hu-PBMC-NOG mice. As described above, the PBMC transplanted to NOG mice were intensely activated in the xenogeneic environment and had undergone ~4 cycles of proliferation by day 2; a majority of the cells had undergone ≥10 cycles of proliferation by day 4 (Fig. 3B). These data suggested that R5 HIV-1 might extensively replicate in the hu-PBMC-NOG mice immediately after R5 HIV-1 inoculation. When we collected blood samples on days 5, 9, and 16 following the inoculation and determined R5 HIV-1 RNA copy numbers in infected, saline-treated mice ($n = 7$), the geometric mean copy number was 8.6×10^3/ml (range, 1.7×10^3 to 1.0×10^5) on day 5 and rapidly increased to 1.9×10^5/ml (range, 2.2×10^4 to 3.0×10^6) on day 9; by day 16, the mean copy number had reached 7.7×10^5/ml (range, 2.6×10^5 to 3.0×10^6/ml). However, AK602 significantly suppressed viremia by ~1.1 log, as examined on day 5; the mean numbers of R5 HIV-1 RNA copies in AK602-administered mice were 1.6 and 1.8 logs lower than those in saline-treated mice examined on days 9 and 16, respectively (Fig. 7). Comparable viremia suppression was seen in the mice receiving ddI (Fig. 7). It was noted that although AK602 did not completely prevent the viremia from further increasing after day 5, there was a clear reduction in the viremia increase rates. The mean slopes (change in RNA copies per day over the range of data from 5 to 16 days) for the group receiving saline was 0.167 ± 0.042, whereas those for the AK602 and ddI groups were 0.102 ± 0.041 and 0.091 ± 0.037, respectively. Thus, the rates of increase in the AK602 ($P = 0.0057$) and ddI ($P = 0.0023$) mice were significantly lower than that for the mice given saline, indicating that both of the agents significantly inhibited R5 HIV-1 replication in this mouse model over the range of days evaluated. No apparent AK602- or ddI-associated adverse effects were seen throughout the study period.

DISCUSSION

In the present hu-PBMC-NOG mouse model, human $CD4^+/CD8^+$ cell ratios went down to 0.1 by 16 days after R5 HIV-1 inoculation, the amounts of proviral DNA and p24 gag antigen reached 10^5 to 10^6 copies/10^5 $CD4^+$ cells and 10^5 pg/ml, respectively (Fig. 6), and no mice failed to be infected with R5 HIV-1. It is noteworthy that the use of NOG mice provides a higher engraftment rate than with other SCID mice such as NOD/Shi-SCID mice treated with anti-NK cell antibody or the β_2-microglobulin-deficient NOD-SCID mice (10). With NOG mice, the chimeric rate of 30 to 40% is achieved, and cord blood $CD34^+$ cells have been shown to "take" with as few as 100 cells (10). Moreover, all infected mice developed high levels of R5 HIV-1 viremia by day 16, reaching as high as 10^6 copies/ml (Fig. 7). It is worth noting that the notably high levels of HIV-1 viremia seen in the present mouse model by 16 days after R5 HIV-1 exposure can be seen only on acute infection or up to 10 years after HIV infection in humans (3, 4).

In the present study, we found that the conspicuous susceptibility to the infectivity and replication of R5 HIV-1 in these mice appeared to stem from the hyperactivation of the implanted human PBMC. The implanted PBMC were highly activated in the xenogeneic environment, expressed quite high

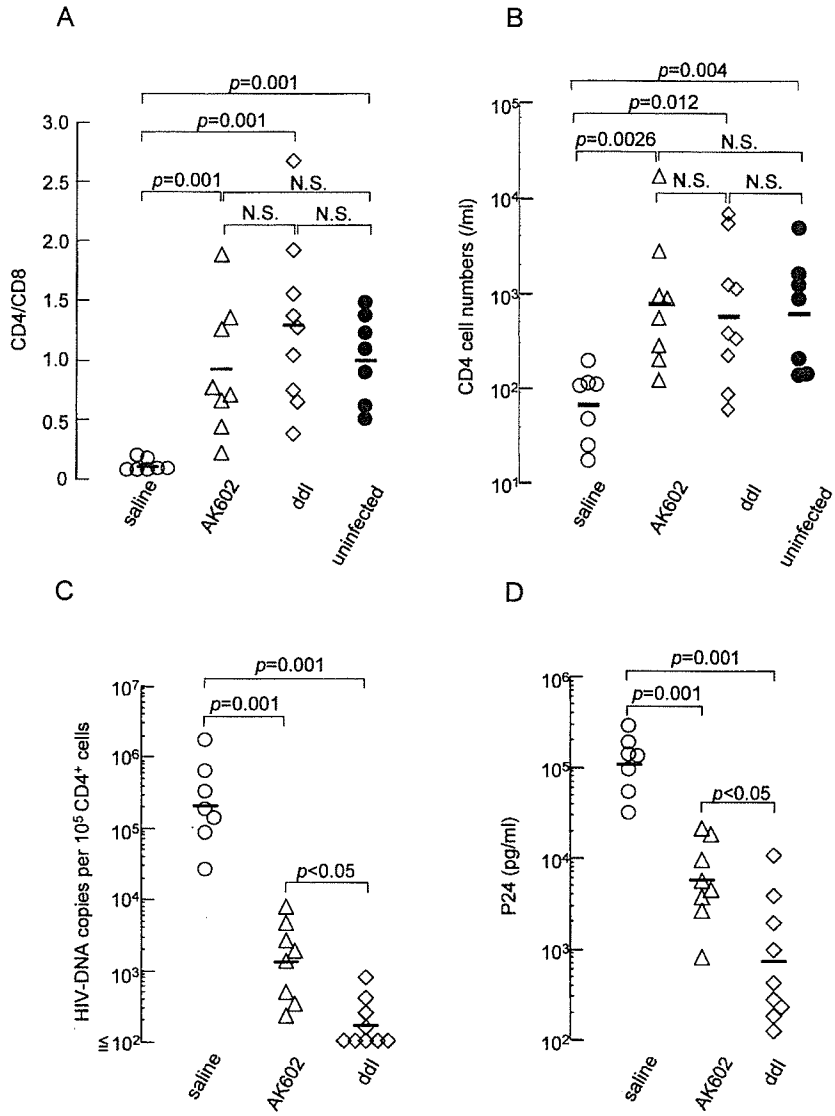

FIG. 6. Effects of AK602 on $CD4^+/CD8^+$ ratios and the amounts of proviral DNA and HIV-1 p24 in infected hu-PBMC-NOG mice. (A) Overall profiles of $CD4^+/CD8^+$ cell ratios. Note that the mean $CD4^+/CD8^+$ cell ratio in mice given saline ($n = 7$) was 0.1, while those in mice given AK602 or ddI were 0.92 and 1.29, respectively. The mean ratio in uninfected mice was 1.0. (B) Numbers of $CD4^+$ cells per microliter in each mouse group. (C) HIV-1 proviral DNA copy numbers in $CD4^+$ cells from each mouse group were determined by real-time PCR assay. Values are shown per 10^5 $CD4^+$ cells, as described in Materials and Methods. Note that the mean number of HIV-1 proviral DNA copies was 2.0×10^5 per 10^5 $CD4^+$ cells in mice given saline, while those in AK602- and ddI-treated groups were 1.3×10^3 and 1.8×10^2 per 10^5 $CD4^+$ cells (both, $P = 0.001$), respectively. (D) Amounts of plasma p24 antigen. Note that the amounts of p24 in plasma were high in saline-treated mice while AK602 and ddI significantly suppressed the serum p24 amounts as examined on day 16 after $HIV\text{-}1_{Ba\text{-}L}$ inoculation. The short bars indicate the arithmetic (A) and geometric (B, C, and D) means obtained.

levels of HLA-DR, and rapidly and continuously proliferated immediately after intraperitoneal infusion (Fig. 3A, B, and D). Moreover, the implanted PBMC expressed as much as 2.8-fold-higher levels of CCR5 on day 3 following implantation compared to PHA-PBMC on day 3 in culture (Fig. 3E). The combination of rapid proliferation and high levels of CCR5 expression of the implanted PBMC should explain the reason R5 HIV-1 rapidly replicated in the hu-PBMC-NOG mice and presented such high levels of R5 HIV-1 viremia. In this regard, only a few groups to date have documented the levels of viremia in the scientific literature. Among them are those by Garaci et al. (8) and Koyanagi et al. (14). The former documented high levels of viremia with a peak of 2.67×10^6 copies/ml in hu-PBL-NOD-SCID mice in which HIV-1-infected macrophages were inoculated, unlike our NOG mouse model where HIV-1 was directly inoculated. The latter report by Koyanagi et al. does not have viremia data but has data on p24 levels with a geometric mean of 11,092 pg/ml on day 14 after HIV-1 inoculation. However, the variation was much greater (178 to 1,434,444 pg/ml). Thus, one can say that the present model provides a greater reproducibility of high viremia levels than the mouse system reported by Koyanagi (14). It should be noted that the high levels of viremia and high engraftment rate achieved in this mouse model made it possible to monitor the

TABLE 2. Comparison of HIV-1 proviral DNA in human $CD4^+$ and $CD4^-$ cell fractions[a]

Sample	HIV-1 DNA copies (10^5 cells)		
	SCID-PBMC	$CD4^+$ cells	$CD4^-$ cells
Saline 1	138,858	162,193	461
Saline 2	135,967	117,949	<100
Saline 3	83,863	94,590	<100
AK602 1	3,390	2,300	<100
AK602 2	5,575	4,606	<100
AK602 3	1,925	1,398	<100
ddI 1	301	516	<100
ddI 2	793	1,317	<100
ddI 3	<100	118	<100

[a] HIV-1 proviral DNA copy numbers were determined by real-time PCR assay of unseparated human PBMC and purified $CD4^+$ and $CD4^-$ cells, following recovery from hu-PBMC-NOG mice. Values are shown per 10^5 cells, as described in Materials and Methods.

changes in the viremia levels periodically in the same set of mice without sacrificing them, while most of the previously described SCID mouse models required mice to be sacrificed at each time point of testing (25, 29, 30) or needed further in vitro coculture of the PBMC recovered from the mice with freshly prepared uninfected target cells for an additional period of days (9, 34).

We demonstrated in this study that a novel SDP derivative, AK602, exerted highly potent activity against laboratory and primary R5 HIV-1 strains as well as MDR R5 HIV-1 variant with IC_{50} values of subnanomolar concentrations (Table 1). It should be noted that AK602 represents a novel SDP derivative, which binds to human CCR5 but not to human CXCR4, CCR1, CCR2, CCR3, CCR4 or murine CCR5; blocks the binding of MIP-1α to CCR5 with an extremely high affinity (K_d values of ~3 nM); potently blocks HIV-1-gp120/CCR5 binding; and exerts potent activity against a wide spectrum of laboratory and primary R5 HIV-1 isolates including MDR HIV-1 and HIV-1 strains of various clades with IC_{50} values of 0.2 to 0.6 nM in vitro (K. Maeda, H. Ogata, S. Harada, Y. Tojo, T. Miyakawa, H. Nakata, Y. Takaoka, S. Shibayama, D. Fukushima, J. Moravek, E. Arnold, and H. Mitsuya, 11th Conf. Retrovir. Opp. Infect., abstr. 540, 2004; J. Demarest et al., XV Int. AIDS Conf., abstr. WeOrA1231, 2004). The plasma half-life of AK602 in the hu-PBMC-NOG mice, however, proved to be as short as 29 min when the agent was administered intraperitoneally (Fig. 4A). Considering that AK602 possesses such a high binding affinity to CCR5, we presumed that AK602 could remain on CCR5 for an extended period of time even after the agent was removed from the bloodstream in mice. The high and extensive level of AK602 occupancy observed in PBMC recovered from mice receiving AK602 substantiated this presumption (Fig. 4D). The subsequent in vitro experiment in which $CCR5^+$ MAGI cells were incubated with AK602 but exposed to R5 HIV-1 after the removal of the compound from the culture medium showed that AK602's anti-R5 HIV-1 activity can persist for an extensive period of time even if AK602 is no longer present in the culture (Fig. 4E). It is of note that unlike certain reports of in vivo anti-HIV-1 activity of chemokine antagonists which were administered before HIV-1 inoculation, thus demonstrating prophylactic effects of such agents (9, 30), the present system demonstrates anti-HIV-1 treatment after the establishment of HIV-1 infection, analogous to antiviral therapy in clinical settings.

When highly active antiretroviral therapy exerts its potent antiviral effects in clinical settings, a decrease in HIV-1 viremia is seen often within weeks, ultimately resulting in undetectable viremia; however in the present study, the viremia levels in mice receiving AK602 or ddI continued to increase although the rate of increment significantly declined (Fig. 7). The failure of AK602 and ddI to decrease viremia levels could be due in part to such a rapid viral replication in hyperactivated and proliferating $CD4^+$ cells. As discussed earlier, PBMC recovered from the hu-PBMC-NOG mice were highly positive for CCR5 and HLA-DR (Fig. 3D and E), compared to the levels of activation seen in the same donor's PHA-PBMC. It should be noted, however, that the mean numbers of proviral DNA copies on day 16 in mice receiving AK602 and ddI were 1.3×10^3 and 1.8×10^2 per 10^5 $CD4^+$ cells, respectively (Fig. 6C), suggesting that most $CD4^+$ cells (98.7 and 99.8% on average, respectively) were free of HIV-1 and proliferating in those

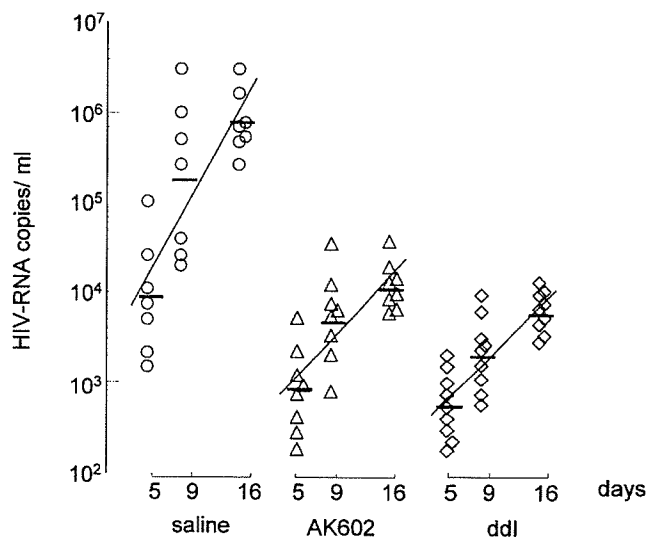

FIG. 7. AK602 suppresses R5 HIV-1 viremia in hu-PBMC-NOG mice. Blood samples were collected on days 5, 9, and 16 after inoculation and were subjected to the determination of R5 HIV-1 RNA copy numbers. Note that the copy numbers in saline-treated mice rapidly increased and reached ~10^6/ml by day 16, while AK602 significantly suppressed the viremia by 1.6 and 1.8 logs as examined on day 9 ($P = 0.001$ compared to saline-treated mice) and day 16 ($P = 0.001$), respectively. Comparable viremia suppression was seen in ddI-treated mice, except on day 16, when ddI activity was greater than that of AK602 ($P = 0.027$). Note that there was a clear reduction in the rate of increase of viremia as well. When the values of $\log_{10}$ HIV-1 RNA copies were calculated and the slopes corresponding to the rates of increase per day were determined, the resulting mean slope (solid line) for the saline-treated mice was 0.167 ± 0.042, whereas those for the AK602- and ddI-treated mice were 0.102 ± 0.041 and 0.091 ± 0.037, respectively. The increase rate for saline-treated mice was significantly higher than those of AK602-treated mice ($P = 0.0057$) and ddI-treated mice ($P = 0.0023$), respectively. The horizontal bars and solid lines represent the geometric means of HIV-1 RNA copy numbers and the slopes calculated, respectively.